The High-Q^2 Form Factor Program at Jefferson Lab

Andrew Puckett

University of Connecticut

CIPANP 2018: Thirteenth Conference on the Intersections of Particle and Nuclear Physics

Outline

- Introduction: Nucleon Elastic Electromagnetic Form Factors (EMFFS): definitions and formalism
- Current experimental status of proton and neutron FFs at large Q^2
- Highlights of nucleon EMFF program in the 11 GeV era of CEBAF
  - Hall A G_{Mp} measurement
  - CLAS G_{Mn} experiment
  - Super BigBite Spectrometer (SBS) FF program: $G_{Mn} + G_{En} + G_{Ep}$
- Prospects for EMFF measurements at a future polarized Electron-Ion Collider
- Theory Highlights (time permitting)

Acknowledgements

- CIPANP 2018 organizers for the opportunity to present this research
- SBS and Hall A collaborations
- Support from US Department Of Energy, Office of Science, Office of Nuclear Physics, Award ID DE-SC0014230 (Early Career research program)
- The University of Connecticut and Jefferson Lab for additional research support

Elastic *eN* scattering and form factors: formalism

$$\mathcal{M} = \frac{4\pi\alpha}{q^2}\bar{u}(k')\gamma^\mu u(k) g_{\mu\nu}\bar{u}(p')\left[F_1(q^2)\gamma^\nu + F_2(q^2)\frac{i\sigma^{\nu\alpha}q_\alpha}{2M}\right]u(p)$$

Invariant amplitude for elastic eN scattering in the one-photon-exchange approximation

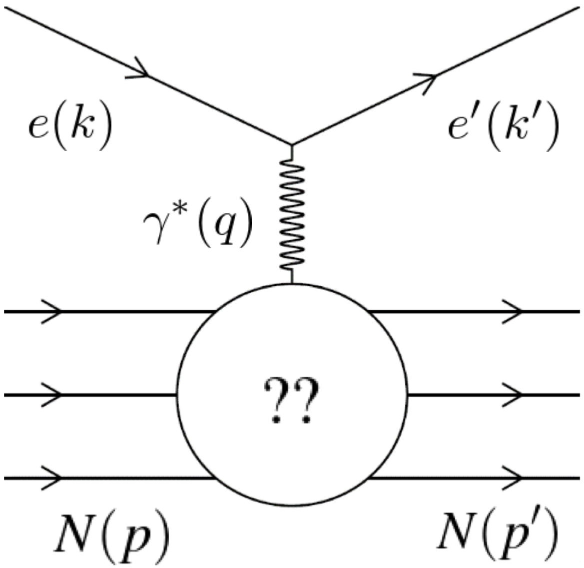

- The most general possible form of the virtual photon-nucleon vertex consistent with Lorentz invariance, parity conservation and gauge invariance is described by two form factors F_1 (Dirac) and F_2 (Pauli):
  - F_1 describes the helicity-conserving amplitude (charge and Dirac magnetic moment)
  - F_2 describes the helicity-flip amplitude (anomalous magnetic moment contribution)

$$\begin{aligned} G_E &\equiv F_1 - \tau F_2 \\ G_M &\equiv F_1 + F_2 \\ \tau &\equiv \frac{Q^2}{4M^2} \end{aligned}$$

Sachs Form Factors G_E (electric) and G_M (magnetic), are experimentally convenient linearly independent combinations of F_1, F_2

$$\begin{aligned} \frac{d\sigma}{d\Omega_e} &= \frac{4\alpha^2 {E'_e}^2 \cos^2\frac{\theta_e}{2}}{Q^4}\left(\frac{E'_e}{E_e}\right)\left[\frac{\epsilon G_E^2 + \tau G_M^2}{\epsilon(1+\tau)}\right] \\ \epsilon^{-1} &= 1 + 2(1+\tau)\tan^2\left(\frac{\theta_e}{2}\right) \end{aligned}$$

Differential cross section in the nucleon rest frame:
Rosenbluth formula

$$\sigma_R \equiv \frac{\varepsilon(1+\tau)\frac{d\sigma}{d\Omega_e}}{\left(\frac{d\sigma}{d\Omega_e}\right)_{Mott}} = \varepsilon G_E^2 + \tau G_M^2$$

Rosenbluth Separation Method: Measure cross section at fixed Q^2 as a function of ε to obtain G_E^2 (slope) and G_M^2 (intercept).

Rosenbluth Separation Method

- The nucleon structure-dependent part of the cross section factorizes from the "point-like" part.
- The "reduced cross section" σ_R depends linearly on ϵ for a given Q^2, with slope G_E^2 and intercept τG_M^2.
- Experimentally, one measures $d\sigma/d\Omega$ while varying the beam energy and scattering angle to change ϵ while holding Q^2 constant

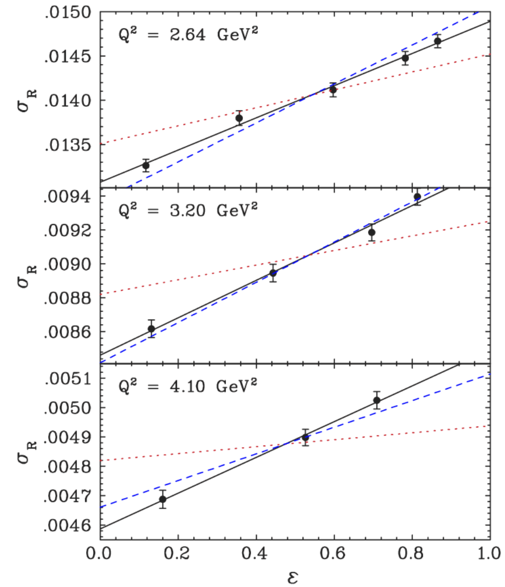

FIG. 2 (color online). Reduced cross sections as a function of ε. The solid line is a linear fit to the reduced cross sections, the dashed line shows the slope expected from scaling ($\mu_p G_E/G_M = 1$), and the dotted line shows the slope predicted by the polarization transfer experiments [6].

Qattan *et al.*, **Phys. Rev. Lett.** 94, 142301 (2005)

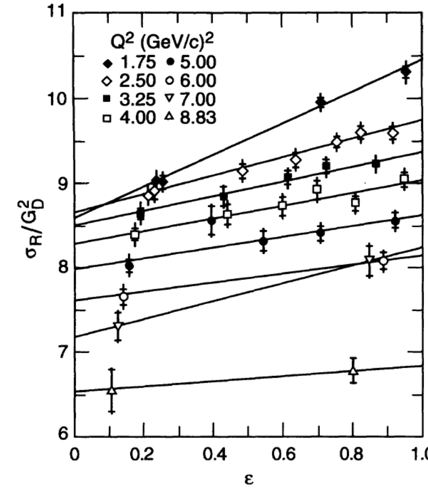

FIG. 22. Reduced cross sections divided by the square of the dipole fit plotted versus ϵ for each value of Q^2. The 1.6 GeV data points correspond to the leftmost point on each line, and the E136 data point is the rightmost point on the Q^2 = 8.83 (GeV/c)^2 line. The inner error bars show the statistical error, while the outer error bars show the total point-to-point uncertainty, given by the quadrature sum of the statistical and point-to-point systematic errors. An overall normalization uncertainty of ±1.77% has not been included.

Andivahis *et al.*, **Phys. Rev. D** 50, 5491 (1994)

$$\frac{d\sigma}{d\Omega_e} = \left(\frac{d\sigma}{d\Omega_e}\right)_{Mott} \frac{\epsilon G_E^2 + \tau G_M^2}{\epsilon(1+\tau)}$$

$$\tau \equiv \frac{Q^2}{4M_p^2}$$

$$\left(\frac{d\sigma}{d\Omega_e}\right)_{Mott} = \frac{\alpha^2 \cos^2\left(\frac{\theta_e}{2}\right)}{4E_e^2 \sin^4\left(\frac{\theta_e}{2}\right)} \frac{E'_e}{E_e}$$

$$\epsilon \equiv \left[1 + 2(1+\tau)\tan^2\left(\frac{\theta_e}{2}\right)\right]^{-1}$$

$$\sigma_R = \epsilon G_E^2 + \tau G_M^2$$

Polarization Transfer in Elastic *eN* scattering

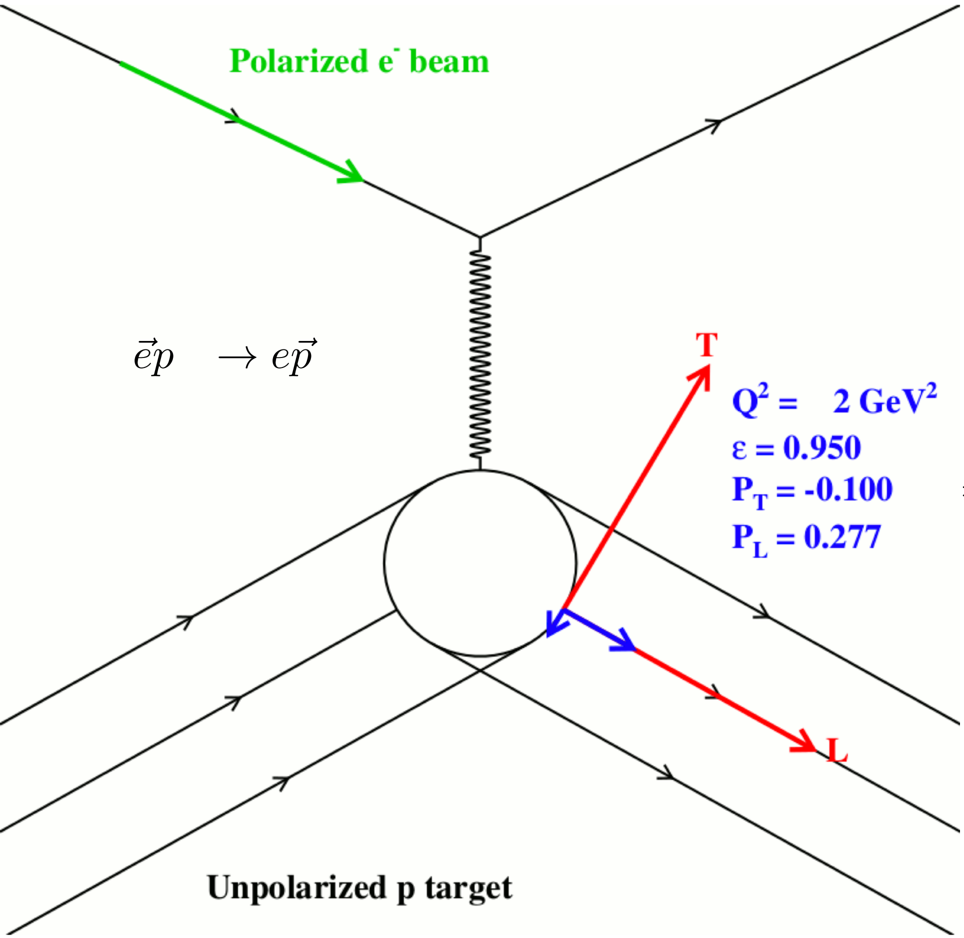

$$
\begin{aligned}
P_t &= -P_{beam}\sqrt{\frac{2\epsilon(1-\epsilon)}{\tau}}\frac{r}{1+\frac{\epsilon}{\tau}r^2} \\
P_\ell &= P_{beam}\frac{\sqrt{1-\epsilon^2}}{1+\frac{\epsilon}{\tau}r^2} \\
P_n &= 0 \\
r &\equiv \frac{G_E}{G_M}
\end{aligned}
$$

$$\Longrightarrow R_p \equiv \mu_p \frac{G_E^p}{G_M^p} = -\mu_p\sqrt{\frac{\tau(1+\epsilon)}{2\epsilon}}\frac{P_t}{P_\ell}$$

- Akhiezer and Rekalo (1968) + Arnold, Carlson, Gross (1981):
  - ***Derived the relations between transferred polarization components in elastic eN scattering and the ratio of electromagnetic FFs $R = \mu G_E/G_M$***
- Perdrisat + Punjabi, 1993 proposal to CEBAF PAC: A ***simultaneous*** measurement of the two recoil polarization components in a polarimeter determines the FF ratio while canceling many systematic uncertainties (beam polarization, analyzing power, FPP instrumental asymmetry)

- ***The ratio of transferred polarization components is directly proportional to G_E/G_M, and therefore much more sensitive to G_E at large Q^2 than the cross section***

Polarized Beam-Polarized Target Asymmetry

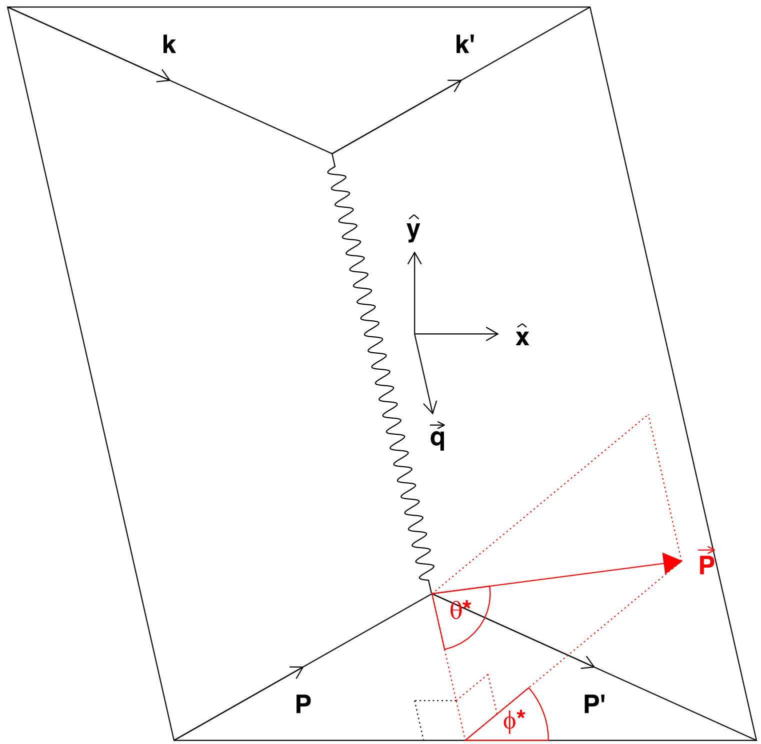

- The beam helicity asymmetry in elastic *eN* scattering from a polarized target is related to the transferred polarization by time reversal symmetry.
- The asymmetry A_t for target polarization perpendicular to the momentum transfer but parallel to the scattering plane ($\theta^* = 90°, \phi^* = 0$) equals the transverse component P_t of the transferred polarization.
- The asymmetry A_ℓ for target polarization along the momentum transfer direction ($\theta^* = 0$) is equal in magnitude but opposite in sign to the longitudinal transferred polarization P_ℓ.
- The sign change between A_ℓ and P_ℓ is due to the proton spin flip required for the absorption of the transversely polarized virtual photon

$$\vec{\mathbf{P}} \equiv \text{Target polarization}$$

$$\begin{aligned} A_{eN} &= -\frac{P_{beam}P_{target}}{1+\frac{\epsilon}{\tau}r^2}\left[\left(\sqrt{\frac{2\epsilon(1-\epsilon)}{\tau}}\sin\theta^*\cos\phi^*\right)r+\sqrt{1-\epsilon^2}\cos\theta^*\right] \\ &\equiv P_{target}\left[A_t\sin\theta^*\cos\phi^* + A_\ell\cos\theta^*\right] \\ A_t &= P_t \\ A_\ell &= -P_\ell \\ A_n &= P_n = 0 \end{aligned}$$

Proton FFs—Rosenbluth data

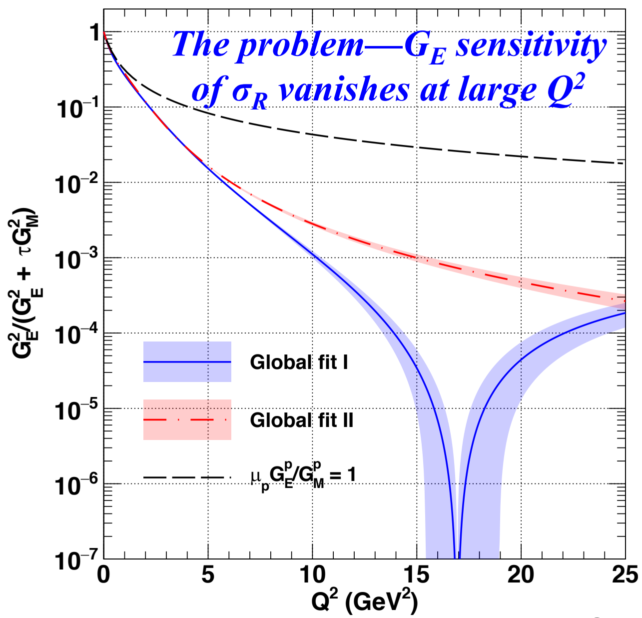

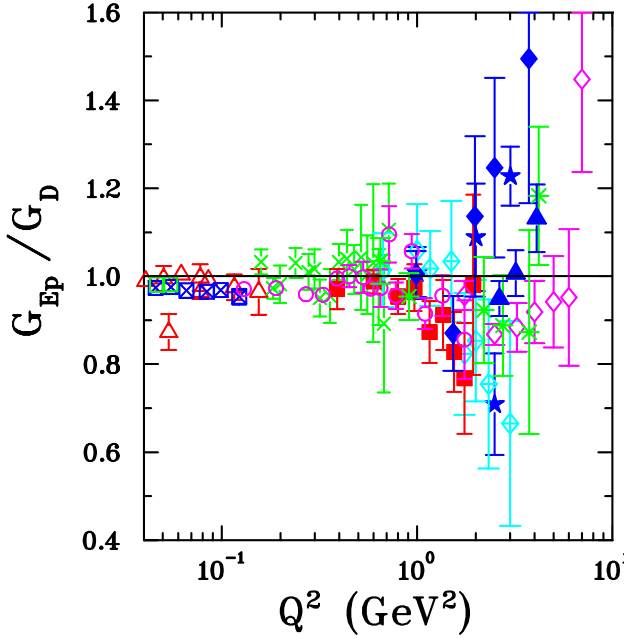

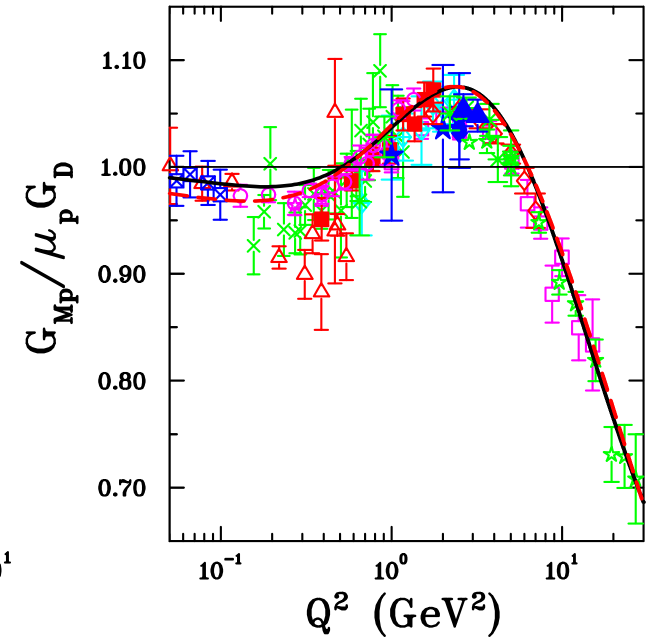

Maximum contribution of G_E^2 term to σ_R vanishes at large τ. Fits to FF data are described in [Phys. Rev. C, 96, 055203 (2017)] (more on these later)

$$\sigma_R = \epsilon G_E^2 + \tau G_M^2$$

G_E^p and G_M^p Rosenbluth Data: $G_E^p \approx \frac{G_M^p}{\mu_p} \approx G_D$

$$G_D \equiv \left(1 + \frac{Q^2}{\Lambda^2}\right)^{-2}$$
$$\Lambda^2 = 0.71 \text{ GeV}^2$$

- Elastic *ep* cross sections have been measured for $0.003 \leq Q^2 \leq 31.2$ GeV².
- Rosenbluth data for G_E^p and G_M^p are qualitatively described by the "dipole" form factor, which is the Fourier transform of a spherically symmetric, exponentially decreasing radial charge/magnetization density.

Proton FFs—Polarization Data

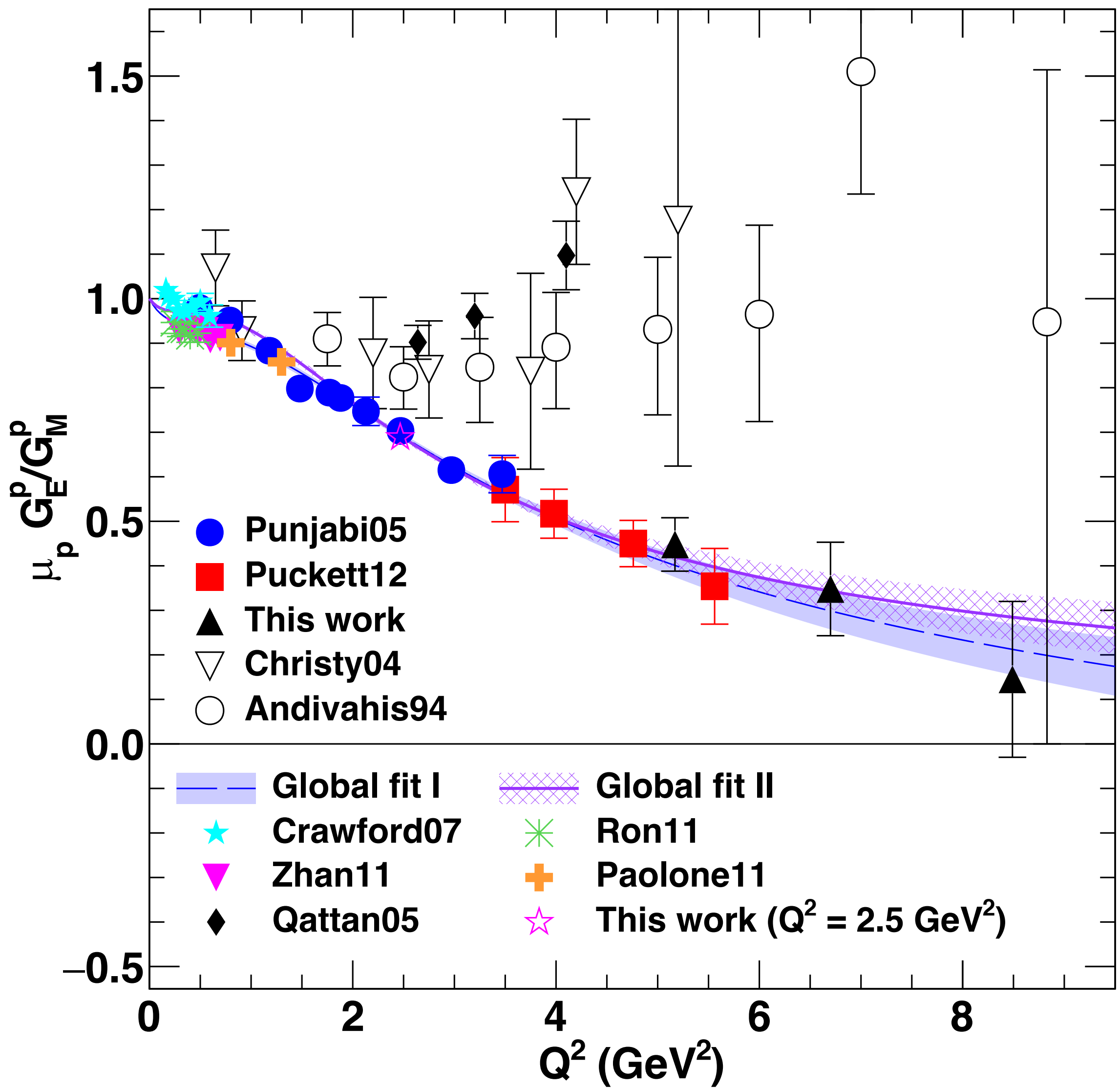

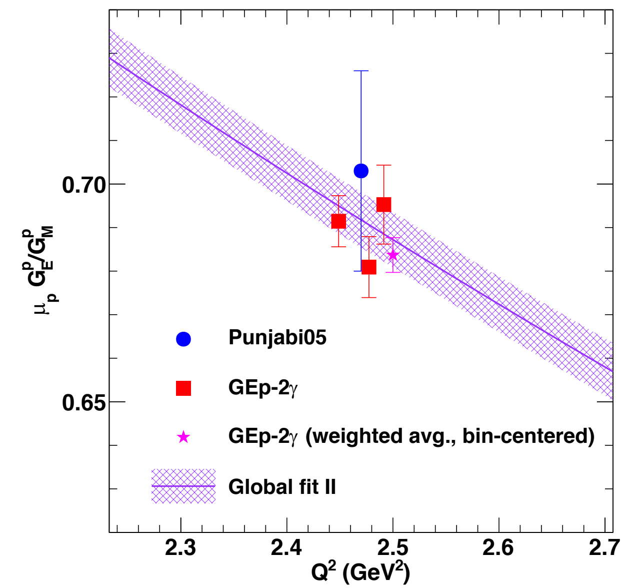

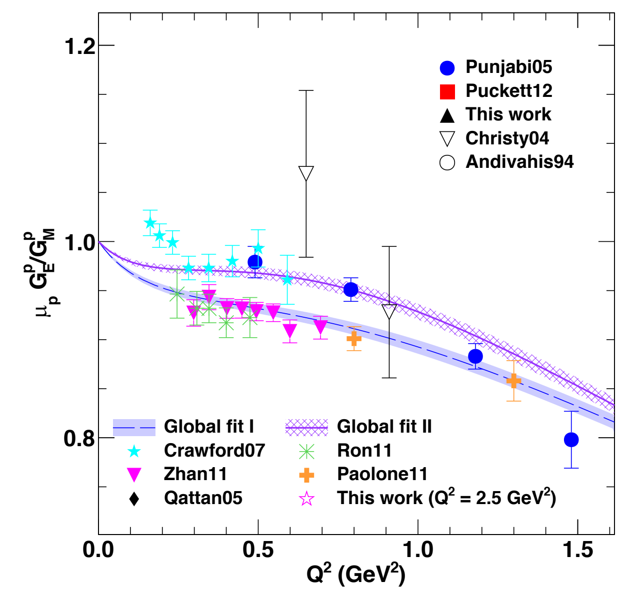

GEp-III/GEp-2γ final results (Puckett *et al.*, [Phys. Rev. C 95, 055203 (2017)])

New "Global" proton FF Fits: Data/fit ratios

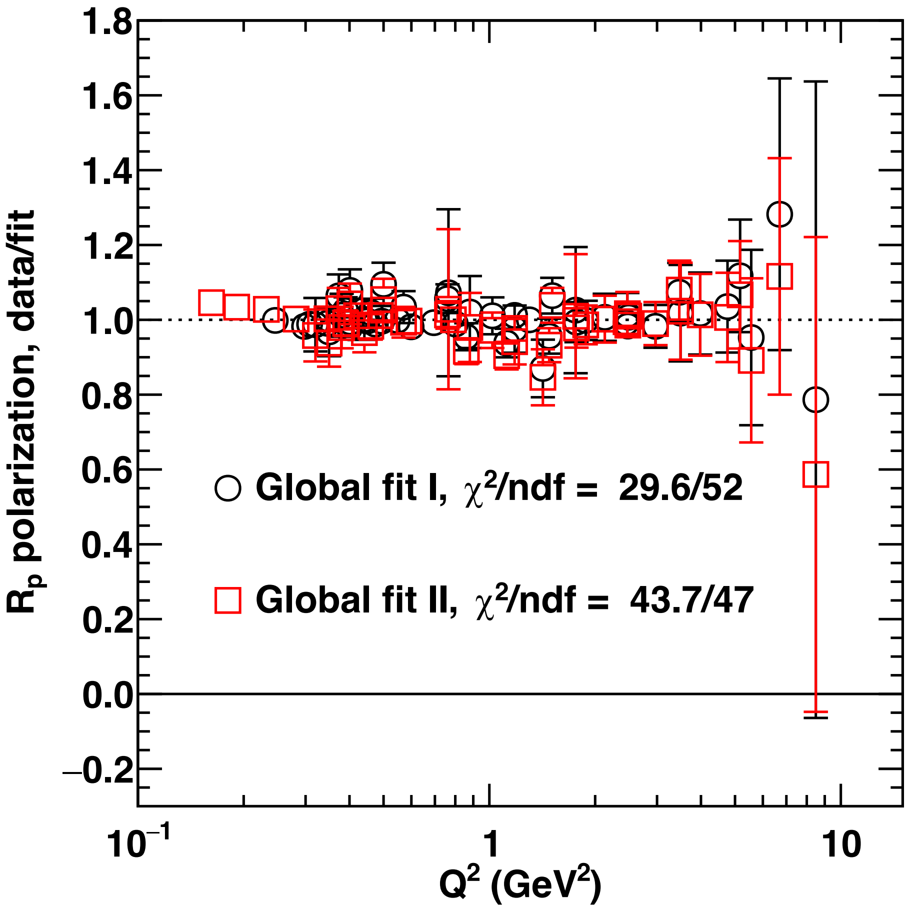

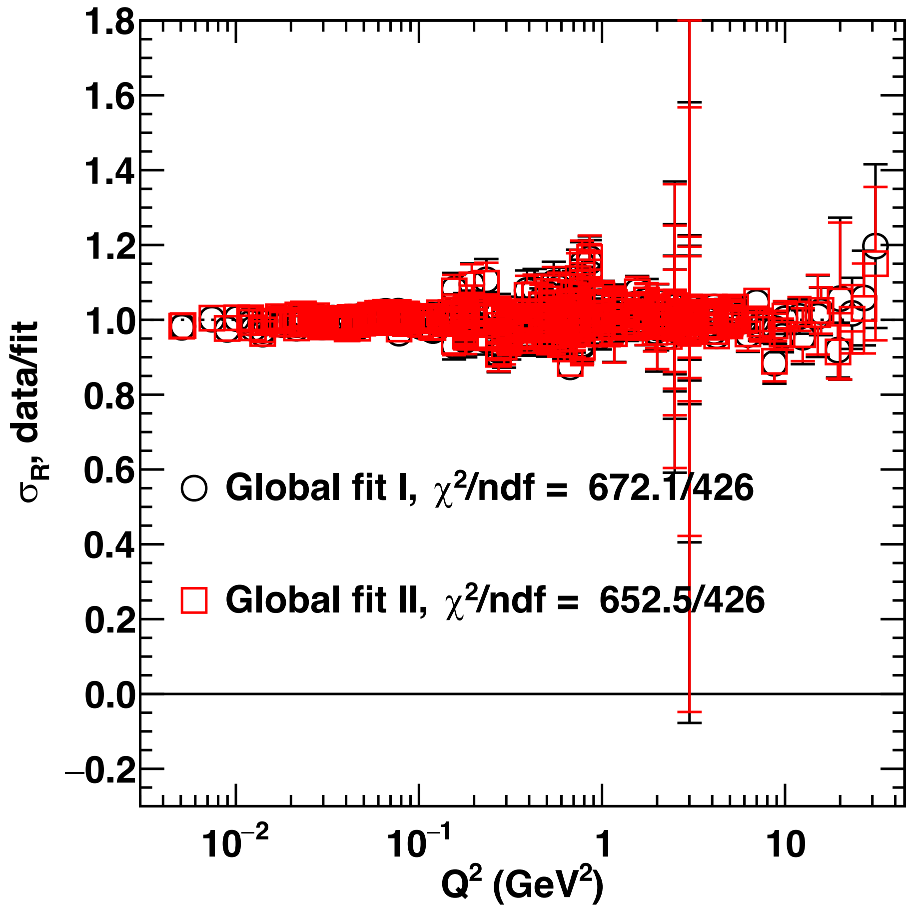

- The global fits described in the appendix of **Puckett *et al.*,** [Phys. Rev. C 95, 055203 (2017)] were used in the analysis described therein to estimate the bin centering effects for the FF ratio at 2.5 GeV^2, and to ensure a self-consistent extraction of P_ℓ / P_ℓ^{Born}.
- The recent Mainz low-Q^2 data (Bernauer *et al.*) were not included in the fits.

Proton FFs compared to data: "Global Fit II"

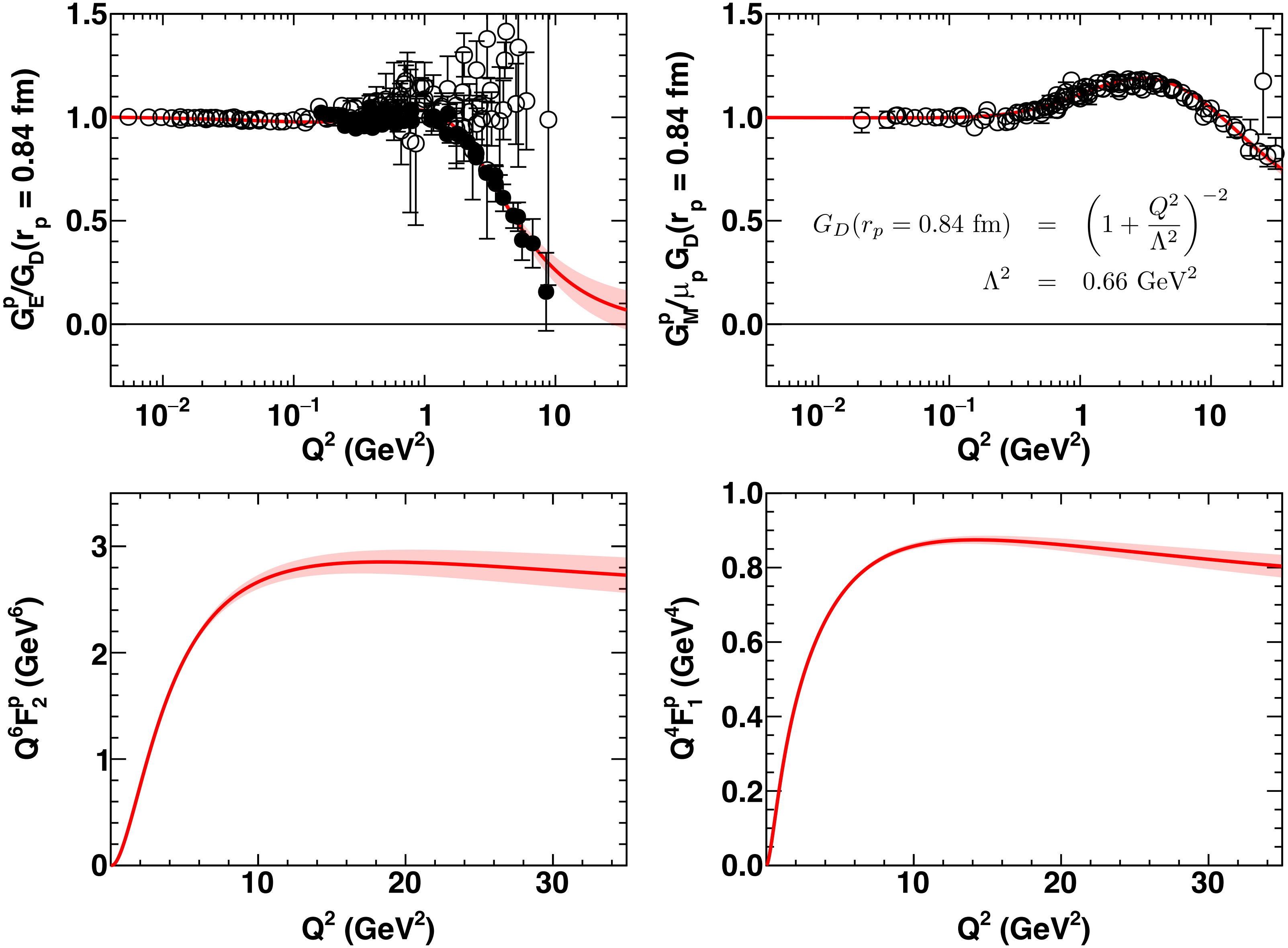

Neutron form factors—G_{Mn} existing data

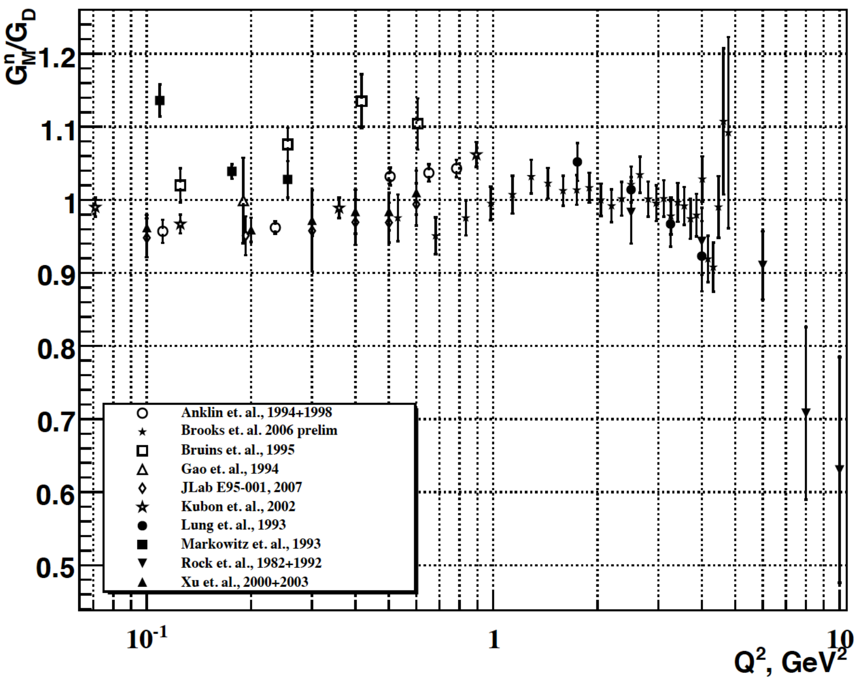

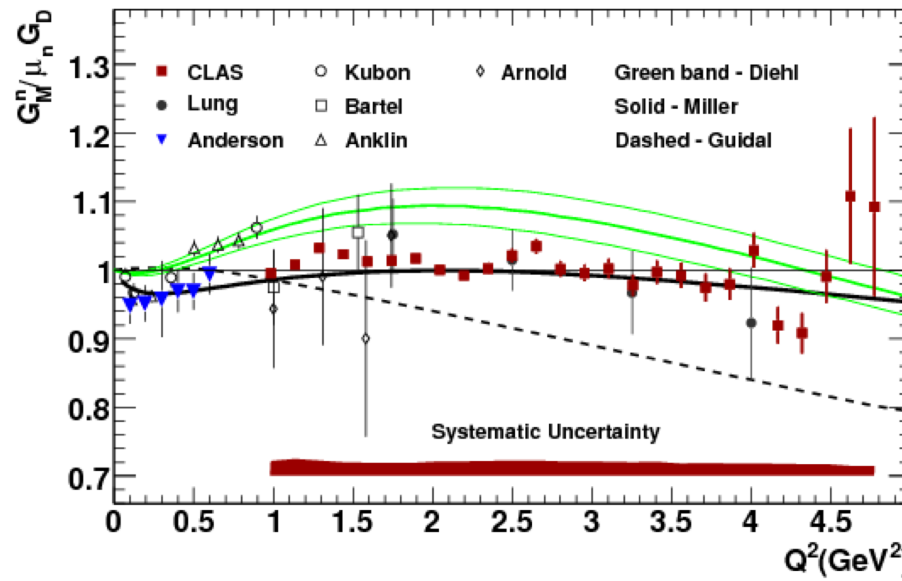

Lachniet *et al.*, CLAS Collaboration, Phys.Rev.Lett. 102 (2009) 192001

- Three main methods have been used to measure G_{Mn}:
  - "Ratio" method: measure cross section ratio of d(e,e'n)p/d(e,e'p)n in quasi-elastic kinematics
  - Absolute d(e,e'n)p quasi-elastic cross section measurement
  - Beam-target double-spin asymmetry* in inclusive quasi-elastic ^{3}He(e,e')

- **Note: double-spin asymmetry method for G_{Mn} would not work for a free neutron target, as the free nucleon asymmetry depends only on the ratio G_E/G_M, and not G_E or G_M independently.*
- Widest combined Q^2 coverage and precision from recent CLAS 6 GeV data from $1 < Q^2 < 5$ GeV^2—consistent with "standard" dipole
- Consistency issues in low-Q^2 data

Neutron form factors—G_{En} existing data

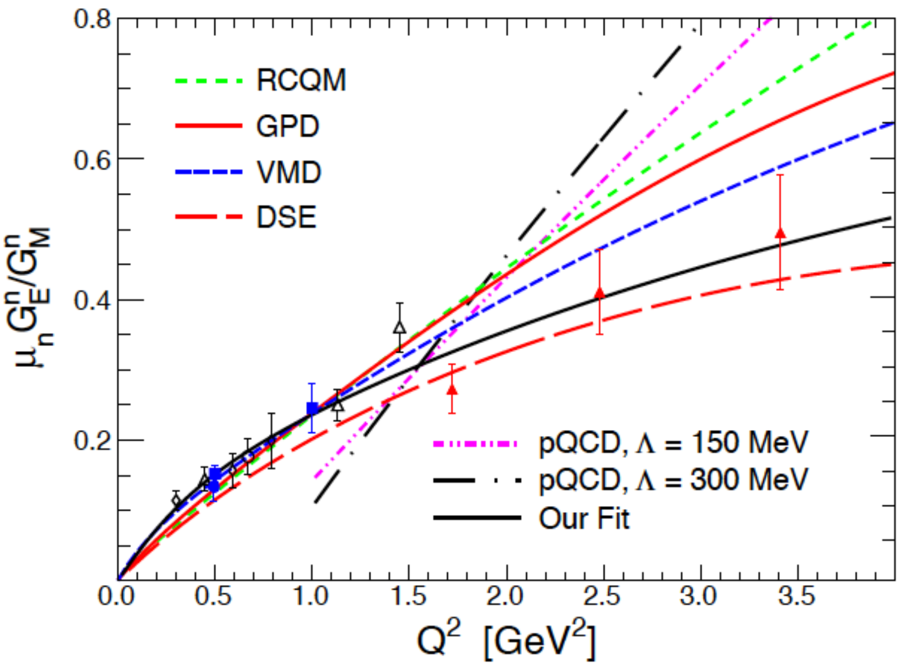

Riordan *et al.*, Phys. Rev. Lett. 105, 262302 (2010)

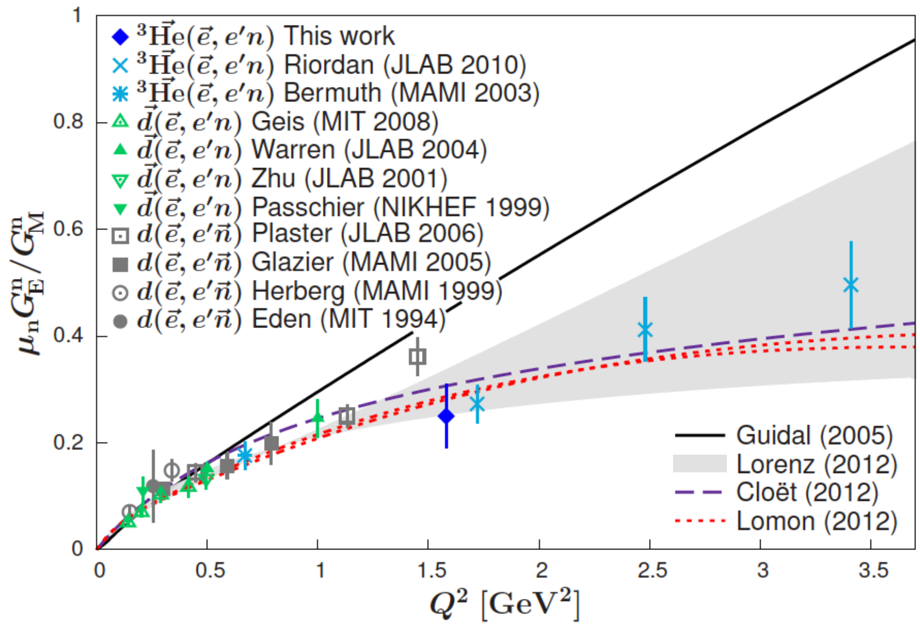

Schlimme *et al.*, Phys.Rev.Lett. 111 (2013), 132504

- G_{En} is the least well-known and most difficult to measure of the nucleon EMFFs:
  - Goes to zero at low Q^2 and cross-section contribution is small at large Q^2
- Existing knowledge is based on polarization observables:
  - Beam-target double-spin asymmetry in semi-exclusive quasi-elastic ^{3}**He**(**e**,e'n)pp
  - Beam-target double-spin asymmetry in semi-exclusive quasi-elastic ^{2}**H**(**e**,e'n)p
  - Neutron recoil polarimetery: d(**e**,e'**n**)p

New! G_{En} at 1.16 GeV^2 from Hall A E02-013

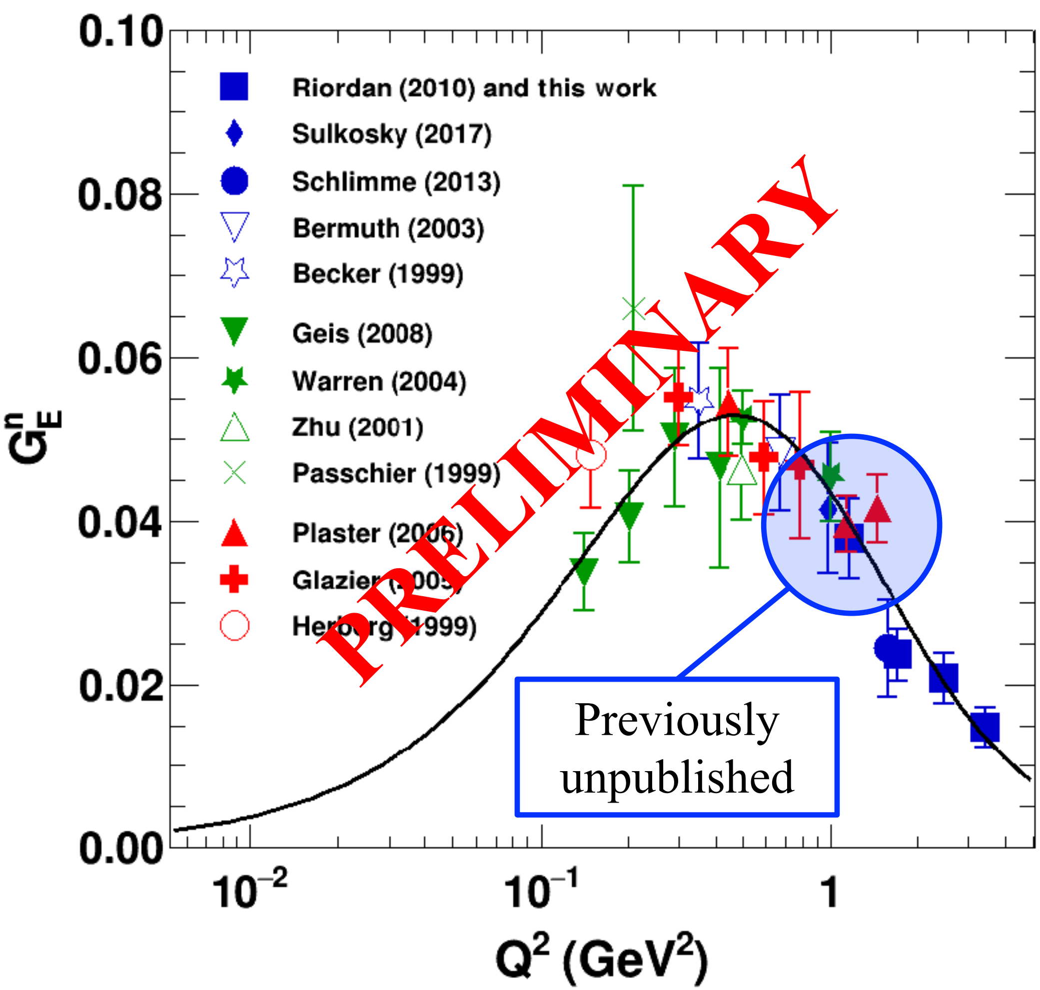

R. F. Obrecht *et al.* (in preparation)

- The last unpublished measurement of G_{En} from E02-013 in JLab's Hall A, which was taken during the commissioning phase of the experiment, was analyzed by UConn Ph.D. thesis student Freddy Obrecht.
- Preliminary result is consistent with Plaster *et al.* deuteron recoil polarization data at similar Q^2
- Analysis essentially complete, up to some debugging of the code used to calculate the nuclear corrections to extract the free neutron asymmetries from measured quasi-elastic on ^{3}He.
- Draft archival paper for the whole experiment (all four Q^2 points), including reanalysis of published measurements, is also nearly complete.

Taking stock of nucleon FF data at the start of JLab 12 GeV

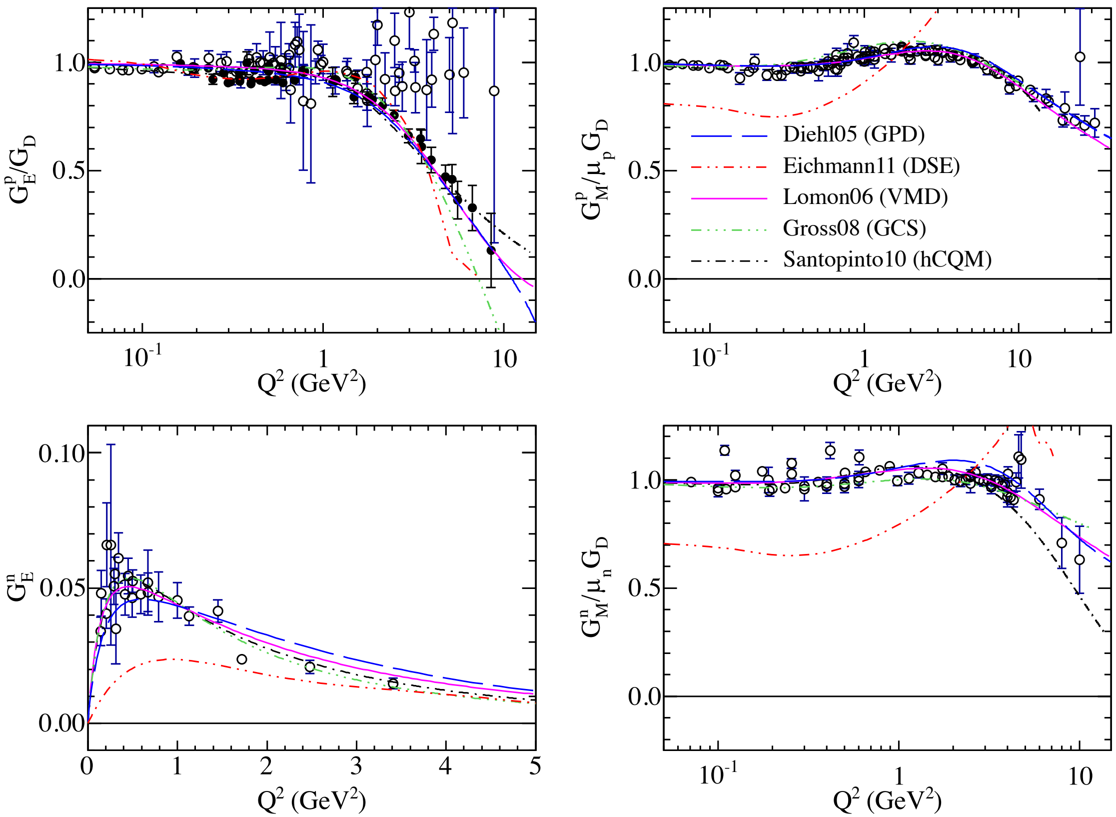

World data for G_{Ep}, G_{Mp}, G_{En}, G_{Mn} compared to selected theoretical model predictions from **Puckett *et al.*, Phys. Rev. C, 85, 045203 (2012)**

$$G_D = \left(1 + \frac{Q^2}{\Lambda^2}\right)^{-2}, \Lambda^2 = 0.71 \text{ GeV}^2$$

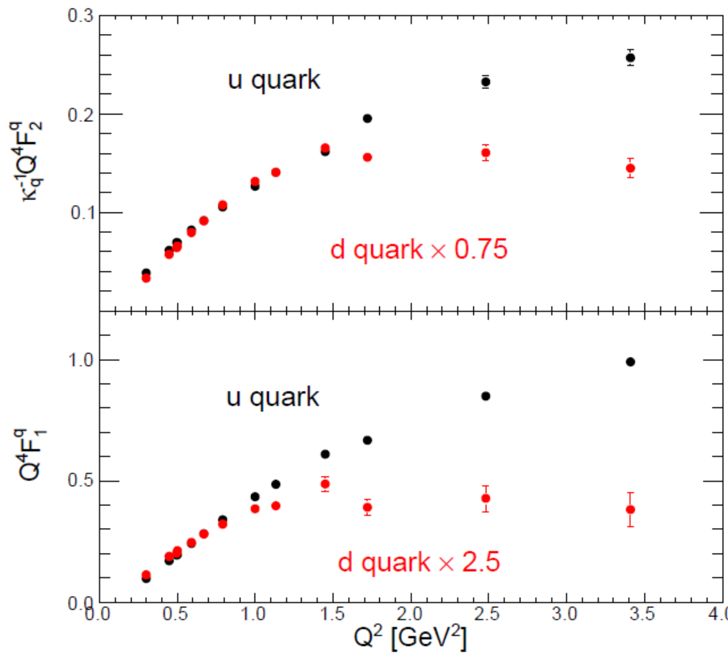

- Flavor decomposition of nucleon FFs: **Cates *et al.*, Phys. Rev. Lett., 106, 252003 (2011)**
- Different behavior of u and d quark contributions to FFs can be interpreted as a probe/signature of diquark correlations

High-Q^2 Nucleon Form Factors in the 12 GeV era of CEBAF

CEBAF @ Jefferson Lab

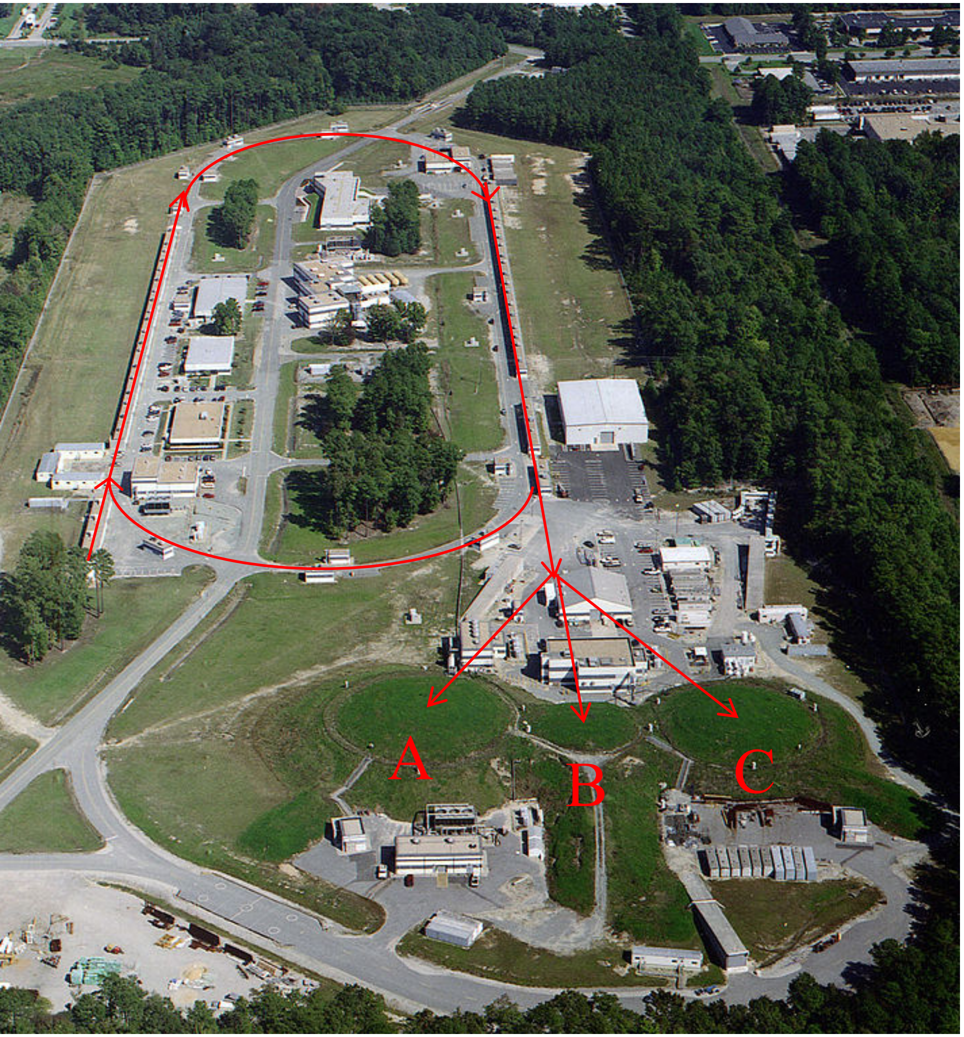

JLab Aerial View

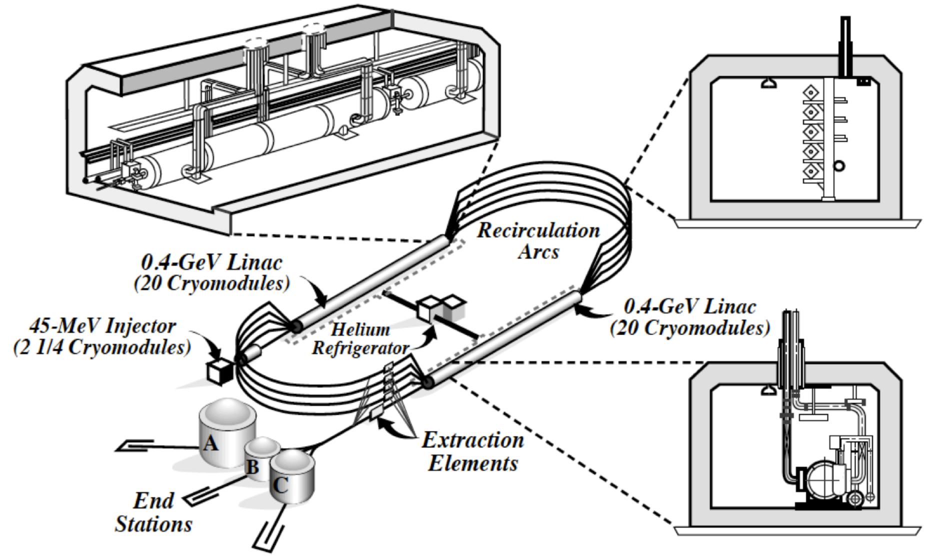

- Superconducting RF electron linacs with up to 5X recirculation
- CW ("100%" duty factor) operation (2 ns bunch period, ~0.3 ps bunch length)
- Polarized source: up to 85-90% polarization
- Three experimental Halls
- Energy up to 6 GeV (upgrade will increase to 11(12) GeV to Halls A/B/C (D))
- Current (up to 180 μA CW)

The 12 GeV Upgrade of CEBAF

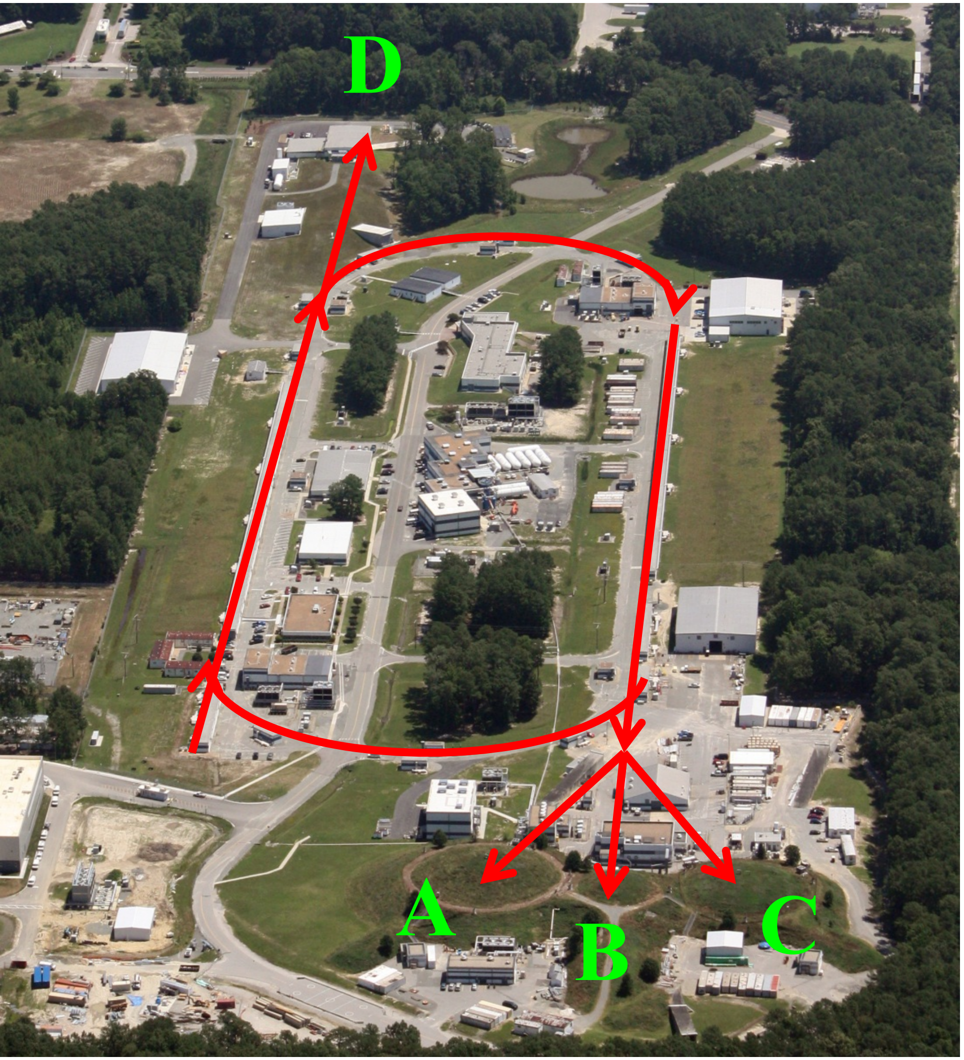

Site Aerial, June 2012

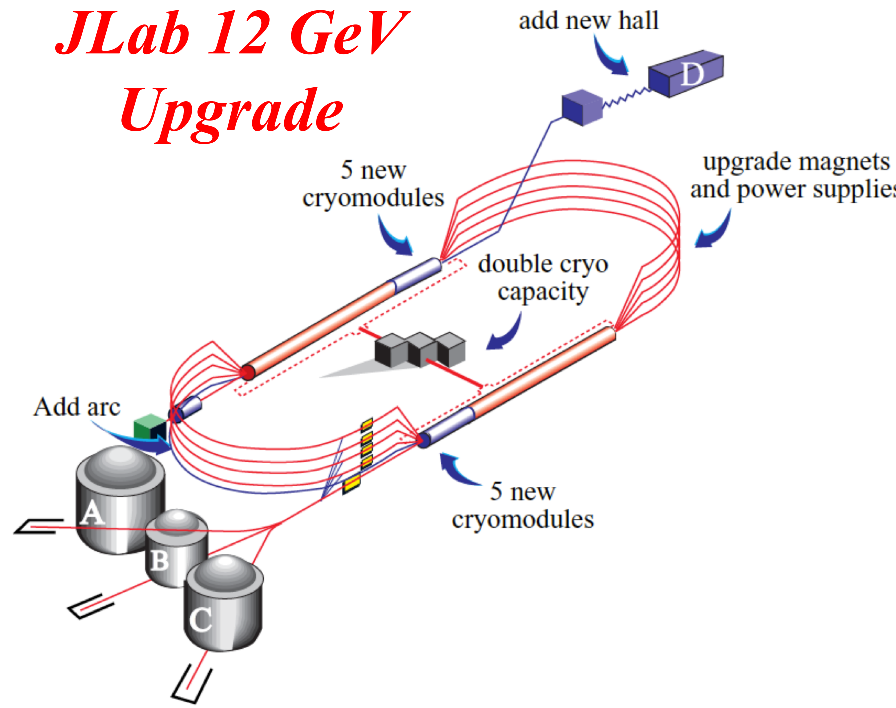

- Superconducting RF electron linacs with up to 5X recirculation
- CW (100% duty factor) operation up to ~80 μA (A+B+C+D)
- Polarized source: up to 85-90% polarization
- Three experimental Halls
- Energy up to 11(12) GeV at 5 (5.5) passes to Halls A/B/C (D)

Electron Scattering Kinematics @11 GeV

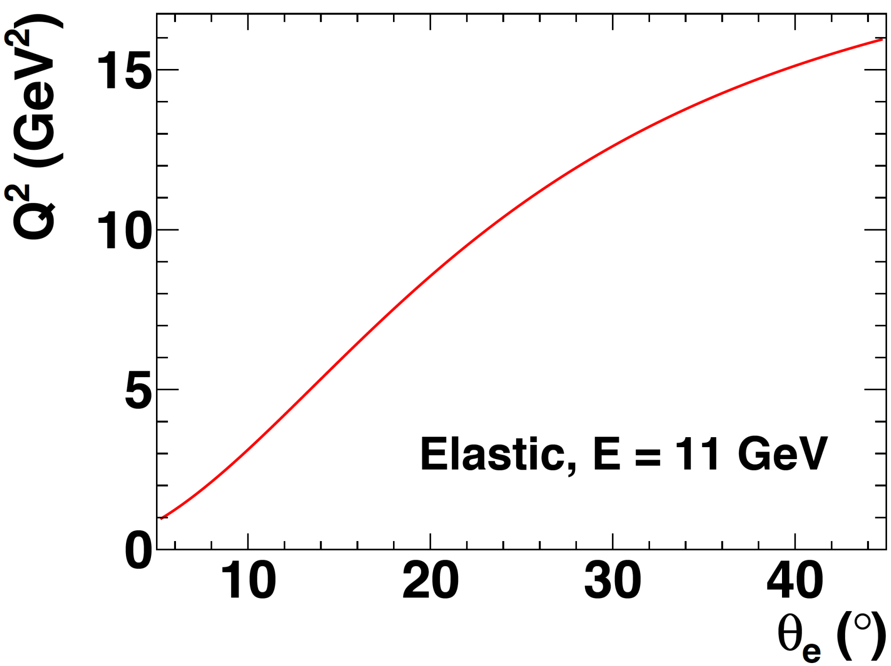

- Measurements of elastic FFs, SIDIS, DVCS, etc involve coincidence N(e,e'X) (electroproduction) reactions, where X =
  - N' (elastic or quasi-elastic)
  - h (SIDIS or DVMP)
  - γ (DVCS)
- Virtual photon angle decreases as "inelasticity" increases:

$$Q^2 = 2M\nu x_{Bj}$$

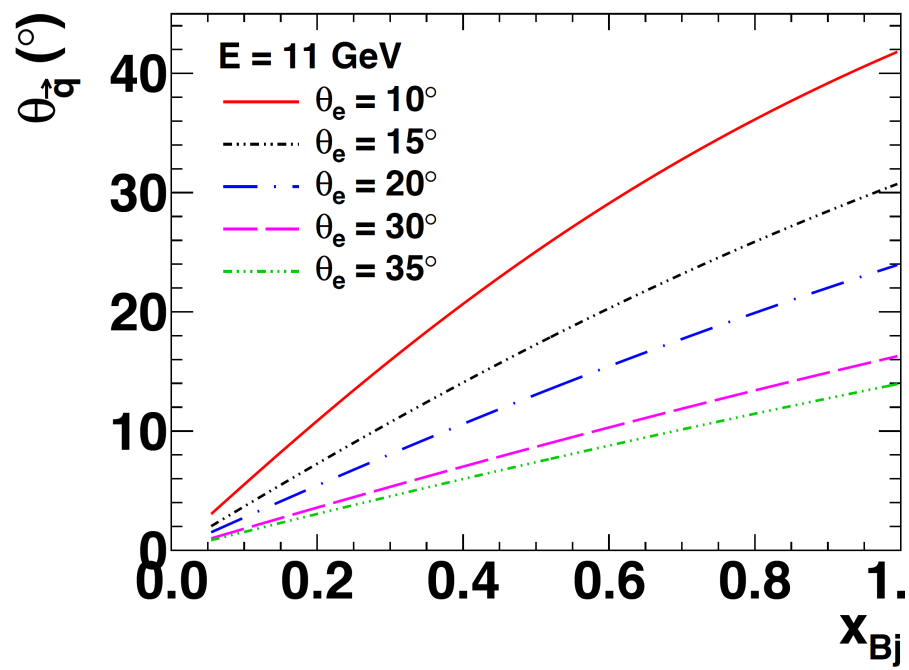

- Particles associated with the partonic (or other) degree of freedom that absorbed the virtual photon are found predominantly near the direction of the momentum transfer **q**
- ***Partonic interpretation of electron scattering data is accessible at large Q^2 → particles of interest are located at forward angles and high momentum***

JLab detector landscape

Figure credit: B. Wojtsekhowski (JLab)

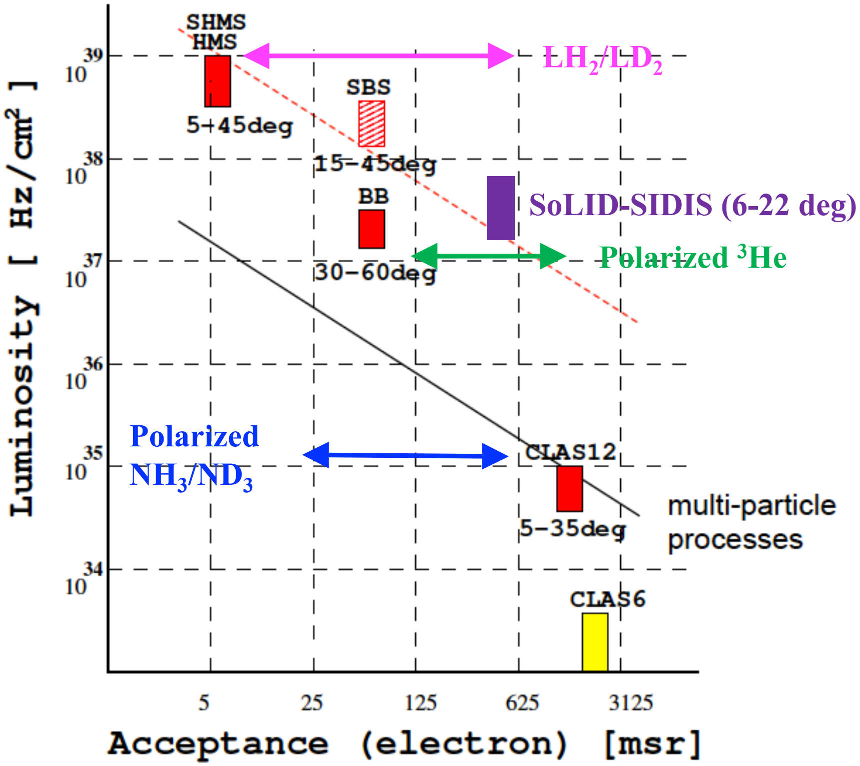

A range of 10^4 in luminosity.

A big range in solid angle:
from 5 msr (SHMS)
to about 1000 msr (CLAS12).
========================

The SBS is in the middle:
for solid angle (up to 70 msr)
and high luminosity capability.

In several A-rated experiments
SBS was found to be the best
match to the physics.

GEM allows a spectrometer
with open geometry (->large
acceptance) at high L.

11/16/15 Super Bigbite Spectrometer Review slide 9

- Complementary equipment/capabilities of Halls A, B, C allow optimal matching of (Luminosity x Acceptance) of the detectors to the luminosity capabilities of the targets, including state-of-the-art polarized target technology.

Precision elastic ep cross sections in Hall A

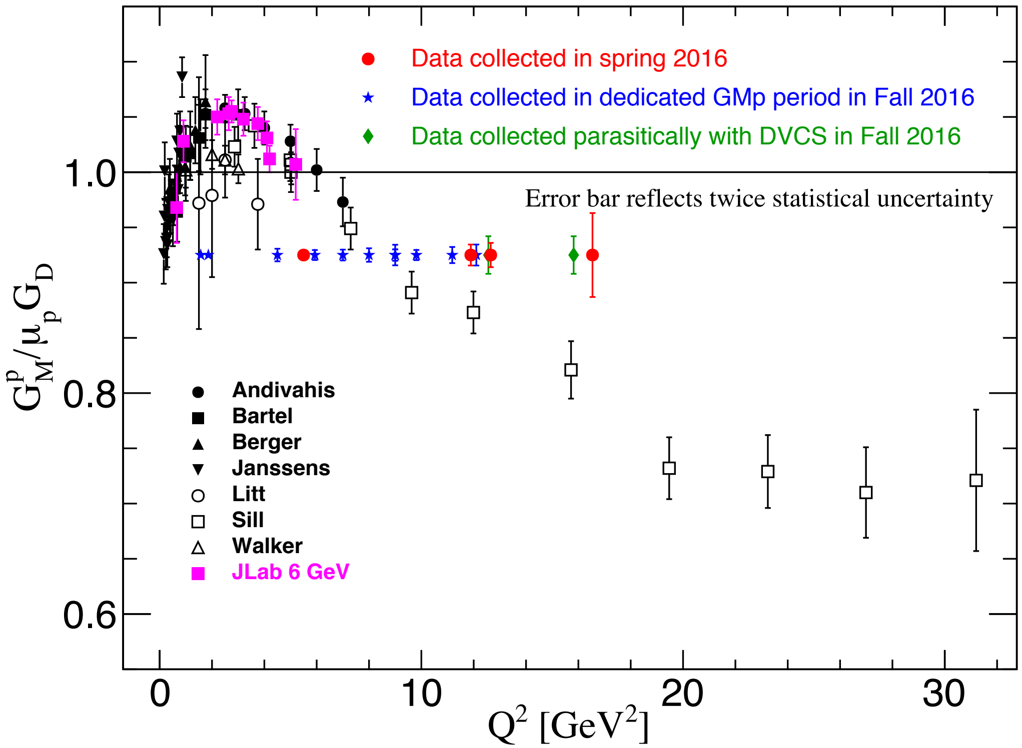

Projected uncertainties from recently completed Hall A high-Q^2 G_{Mp} run: 2018 publication anticipated

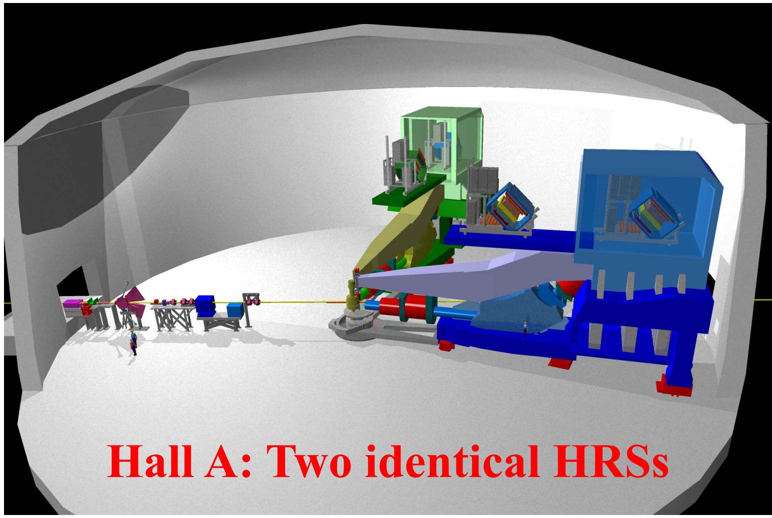

- Elastic ep → ep cross section at large Q^2 is dominated by G_{Mp}.
- Existing data for $Q^2 \geq 10$ GeV^2 come from two SLAC experiments (Kirk *et al.*, Phys. Rev. D **8**, 63 (1973) and Sill *et al.*, Phys. Rev. D, 48(1), 29 (1993)) with large uncertainties
- The absolute elastic *ep* cross section data serve as the "anchor" for the determination of all four nucleon EMFFs

The CLAS12 Spectrometer in Hall B

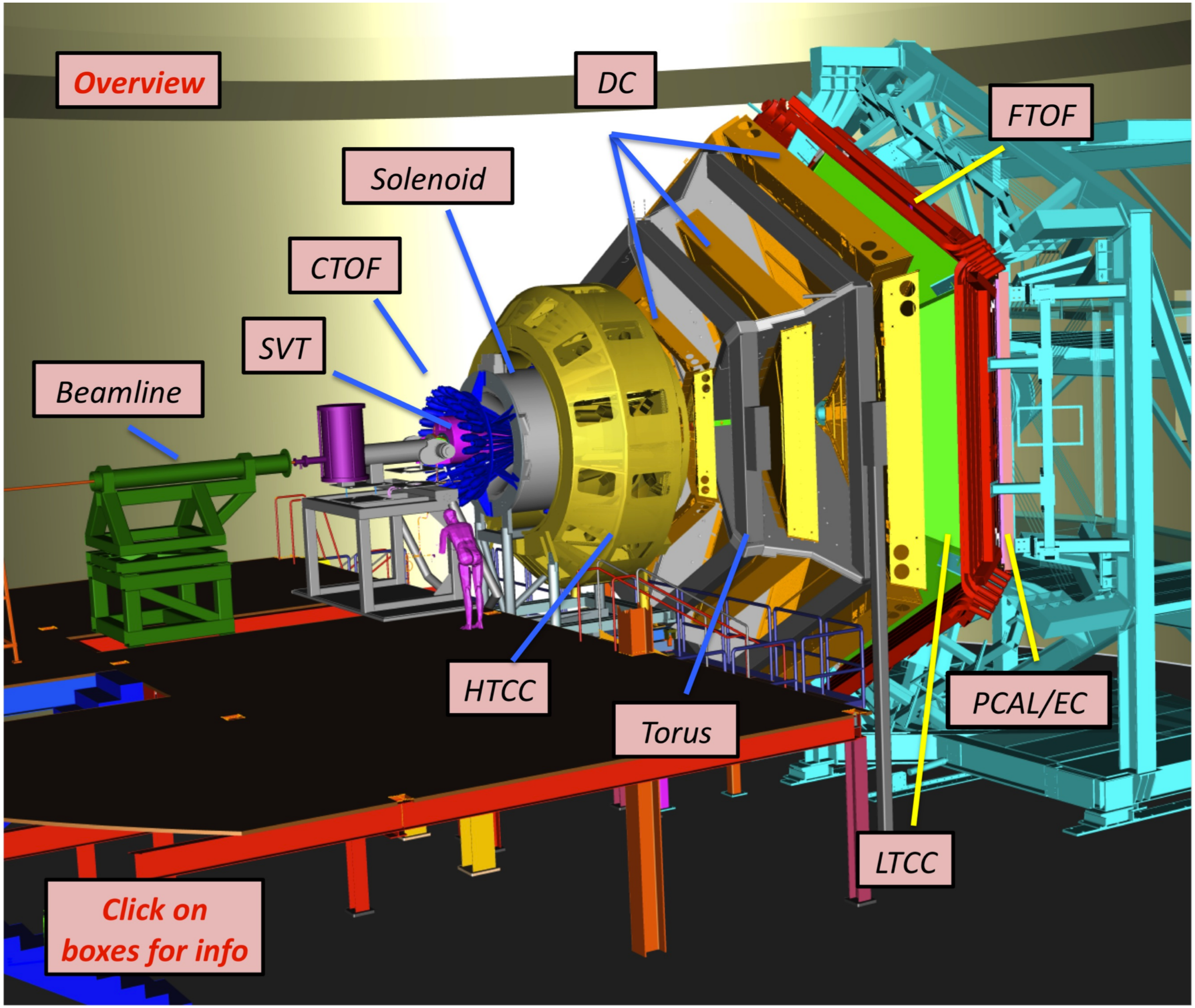

- Large-acceptance, general purpose detector for charged and neutral particles
- Designed to detect multi-particle final states with broad kinematic coverage for exclusive and semi-inclusive reactions at moderately high luminosity
- 5T central solenoid
- Toroidal magnetic field for forward-going particles
- Physics program: GPDs, TMDs, spin, etc.

CLAS12 G_{Mn}: experiment E12-07-104

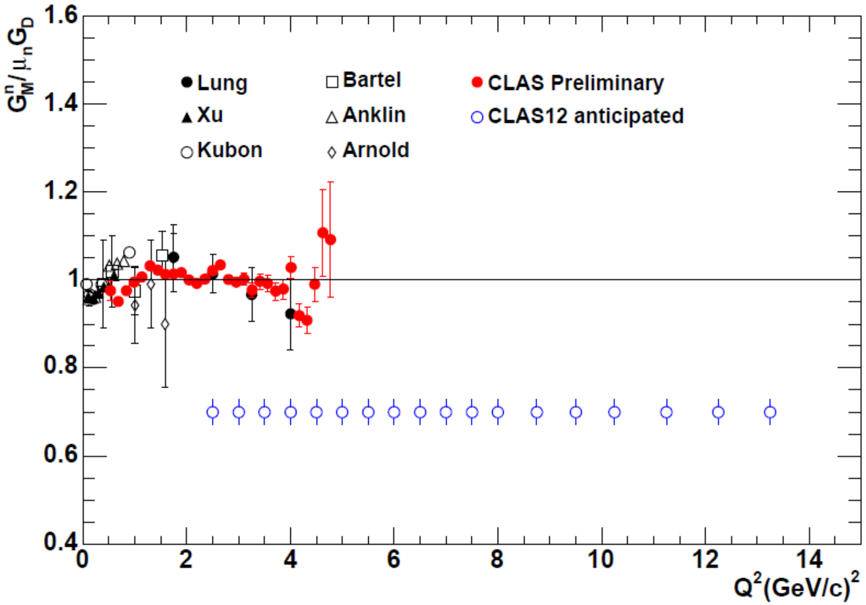

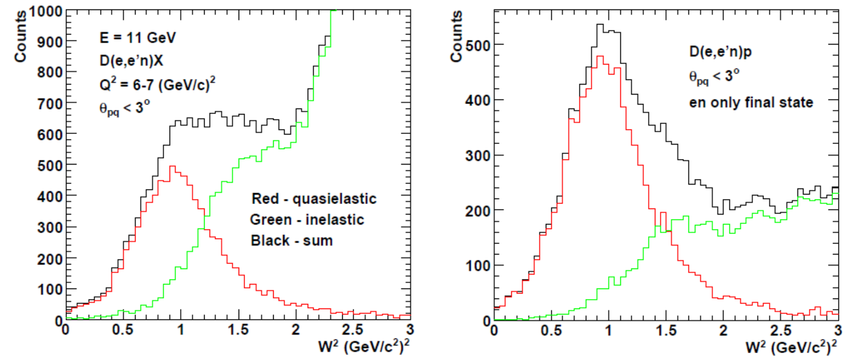

Figure 18: Comparison of the simulated W^2 spectra for the $D(e, e'n)X$ (left-hand panel) and $D(e, e'n)p$ reactions (right-hand panel). Both spectra are for $\theta_{pq} < 3°$.

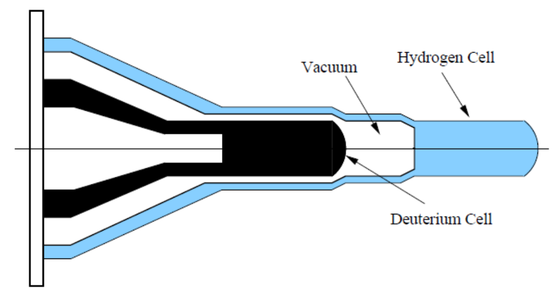

$$R = \frac{\frac{d\sigma}{d\Omega}(D(e,e'n))}{\frac{d\sigma}{d\Omega}(D(e,e'p))}$$

$$R = a(Q^2)\frac{\sigma^n_{mott}({G^n_E}^2 + \frac{\tau_n}{\varepsilon_n}{G^n_M}^2)\left(\frac{1}{1+\tau_n}\right)}{\sigma^p_{mott}({G^p_E}^2 + \frac{\tau_p}{\varepsilon_p}{G^p_M}^2)\left(\frac{1}{1+\tau_p}\right)}$$

- Extract neutron magnetic form factor from the ratio of d(e,e'n)/d(e,e'p) quasielastic cross sections and known form factors of the proton
- Nuclear corrections small at large Q^2
- Important to have independent data (SBS and CLAS12) in high-Q^2 regime to cross-check systematics of G_{Mn}

The Super BigBite Spectrometer in Hall A

Proton form factors ratio, GEp(5) (E12-07-109)

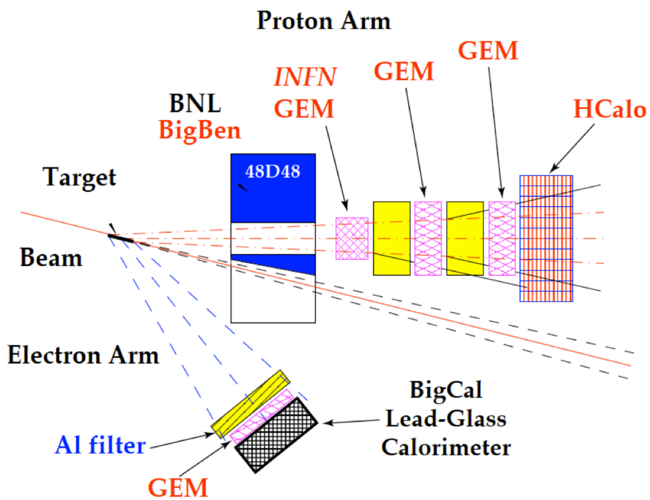

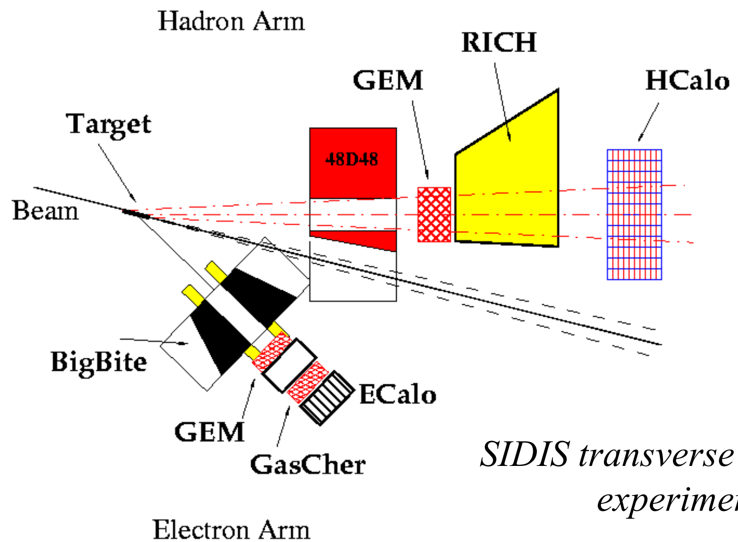

SIDIS transverse single-spin asymmetry experiment: E12-09-018

Neutron form factors, E12–09–016 and E12–09–019

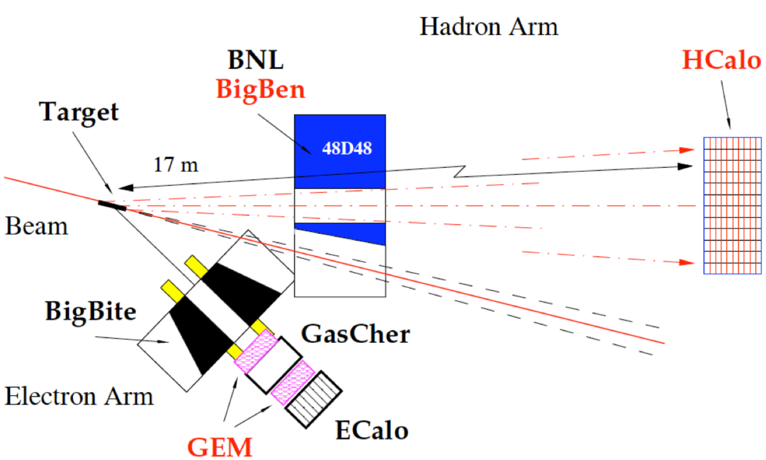

- What is SBS? → A 2.5 T*m dipole magnet with vertical bend, a cut in the yoke for passage of the beam pipe to reach forward scattering angles, and a flexible/modular configuration of detectors.
- Designed to operate at luminosities up to 10^{39} cm^{-2} s^{-1} with large momentum bite, moderate solid angle
- Time-tested "Detectors behind a dipole magnet", two-arm coincidence approach—historically most productive in fixed-target expts.
- ***Large solid-angle + high luminosity @ forward angles = most interesting physics!***

Gas Electron Multipliers (GEMs): High-Rate, High Resolution Charged-Particle Tracking

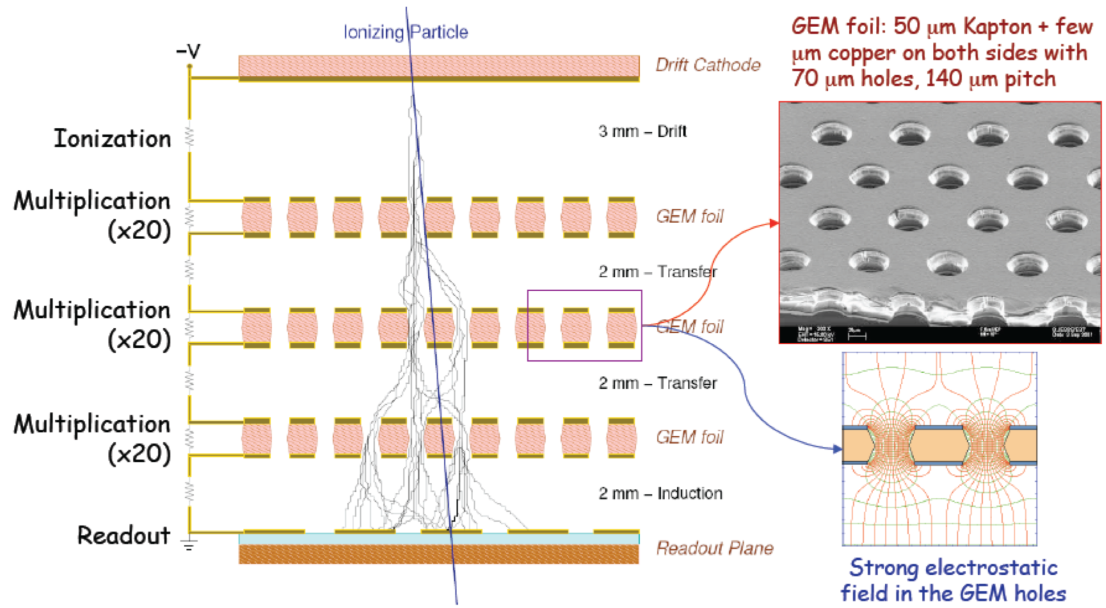

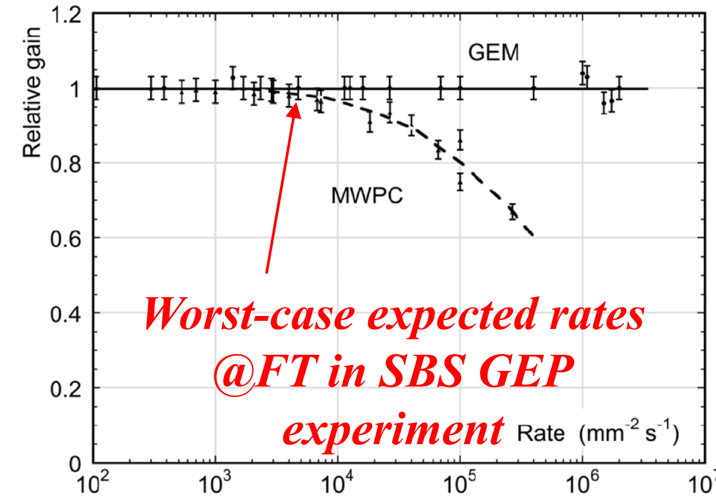

Figure 28.9: Normalized gas gain as a function of particle rate for MWPC [70] and GEM [84].

Stable gain up to very high rates

Recent technology: F. Sauli, NIM A 386, 531 (1997)

- High spatial granularity
- Ability to cascade several foils: higher gain at lower applied voltage, reduced discharge risk
- Readout and amplification stages decoupled
- Excellent spatial resolution ~70 μm
- Fast signals: intrinsic time resolution <10 ns
- **Enabling technology for SBS physics program!**

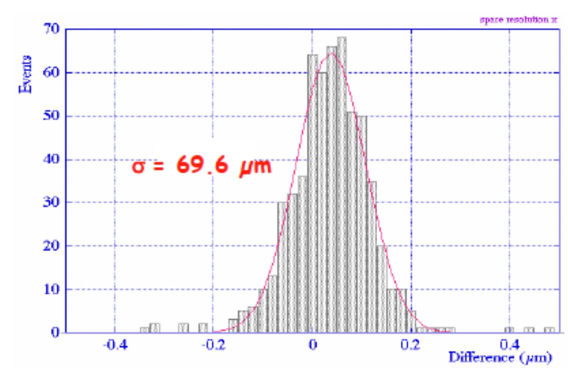

Space resolution

Experiment E12-07-109 (G_{Ep}/G_{Mp} at large Q^2)

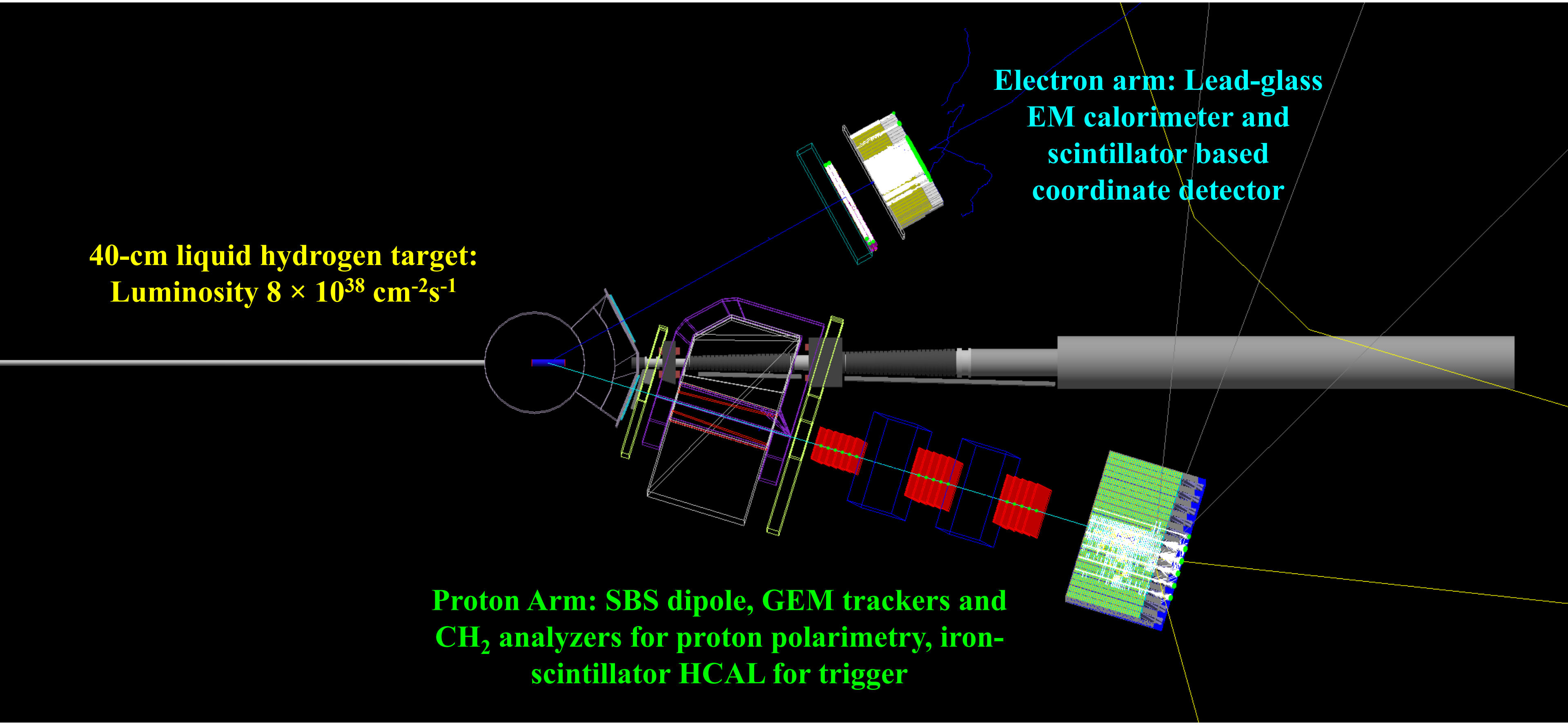

- Original motivation for SBS concept. Need large solid angle to overcome rapidly falling cross section at large Q^2 in elastic *ep* scattering. New double proton polarimeter with GEM-based tracking and hadronic calorimeter-based trigger
- Lead-glass electromagnetic calorimeter to detect the scattered electron in coincidence (using two-body kinematic correlations to aid tracking in high-rate environment and reject inelastic background events); also provides a selective trigger for high-energy electrons.

SBS G_E^p Projected Results

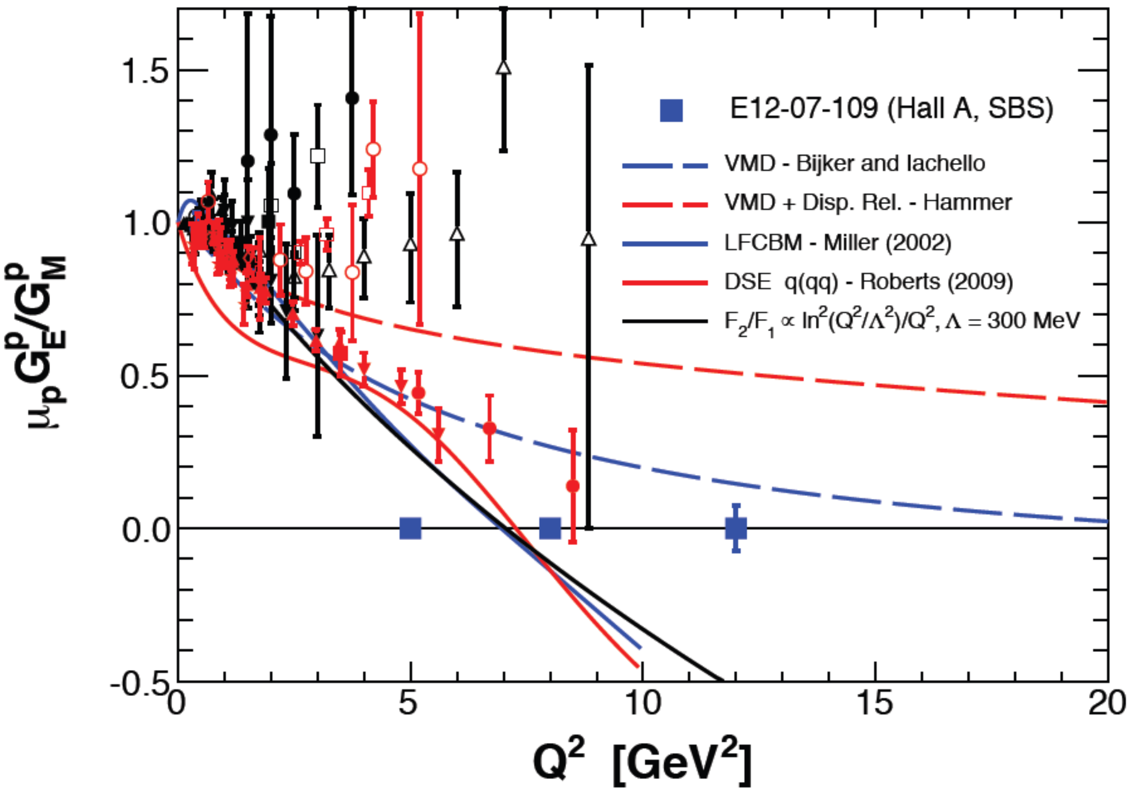

- The SBS GEP experiment in ~11 days running will dramatically improve the statistical precision in $\mu G_E/G_M$ at Q^2 in the range overlapping GEp-II/III, and in 30 days will reach comparable precision at 12 GeV^2 to that of GEp-II/III at 5-6 GeV^2
- Data of such precision carry significant discovery potential and may (or may not) settle the questions of a zero crossing of G_E^p and the onset (or lack thereof) of dimensional scaling.

- Combined with GEN, GMN, GMP experiments, full flavor decomposition of F_1 and F_2 becomes possible up to 10 GeV^2

Kinematics and expected accuracy							
E (GeV)	Q^2 (GeV^2)	θ_E (deg)	P_e (GeV)	Θ_p (deg)	P_p (GeV)	Days	$\Delta\mu G_E/G_M$
6.6	5.0	25.3	3.94	29.0	3.48	1	0.023
8.8	8.0	25.9	4.54	22.8	5.12	10	0.032
11.0	12.0	28.2	4.60	17.4	7.27	30	0.074

Experiment E12-09-019 (G_{Mn} at large Q^2)

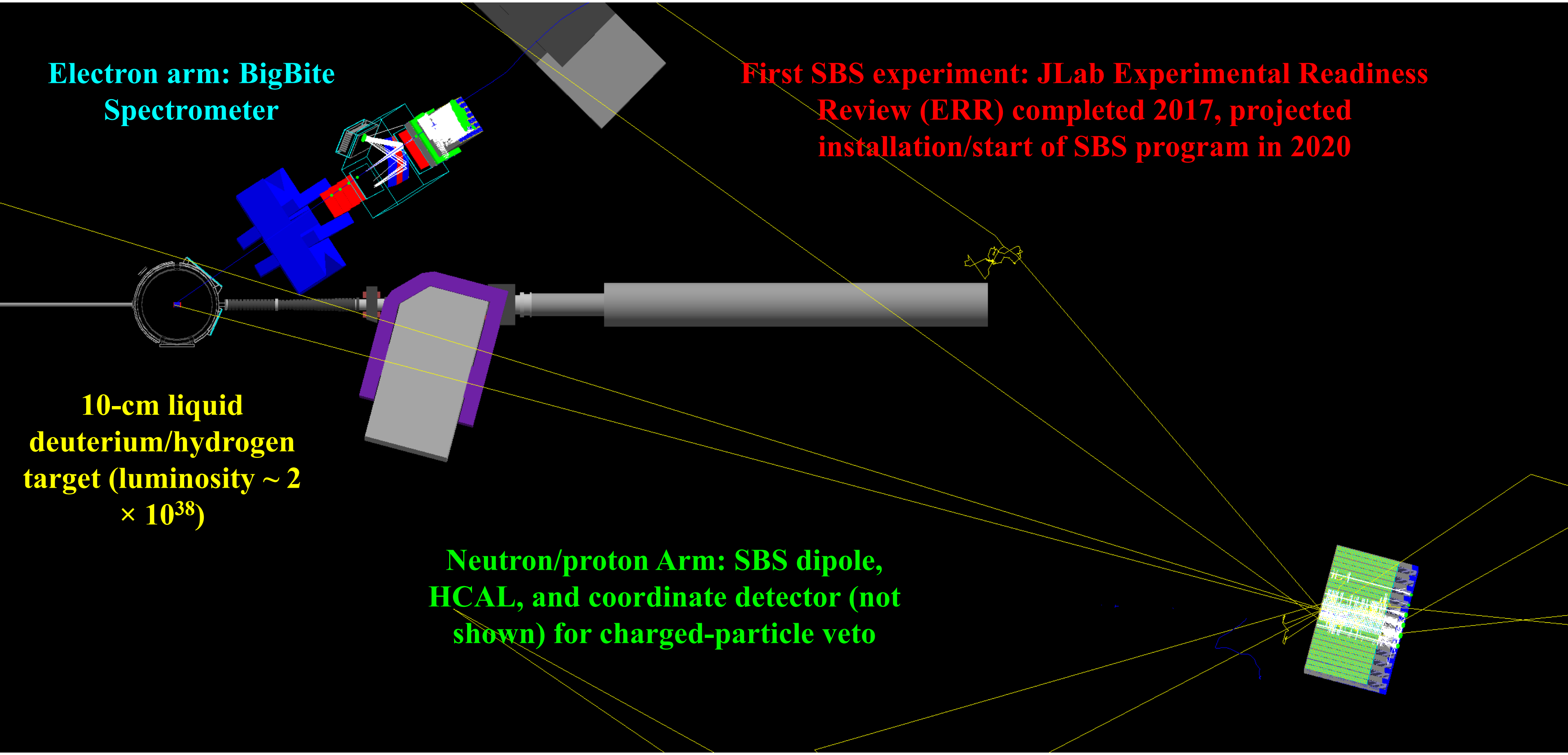

- Neutron magnetic form factor at large Q^2 is obtained from the ratio of quasi-elastic d(e,e'n)p/d(e,e'p)n cross sections on a deuterium target and precise knowledge of elastic ep cross section
- SBS dipole deflects protons to separate from neutrons (relative to $\vec{q}$ vector); nucleon momentum is measured using time-of-flight method to separate quasi-elastic/inelastic channels.
- Existing BigBite spectrometer with upgraded detector package detects the scattered electron.

SBS G_{Mn} projected Results

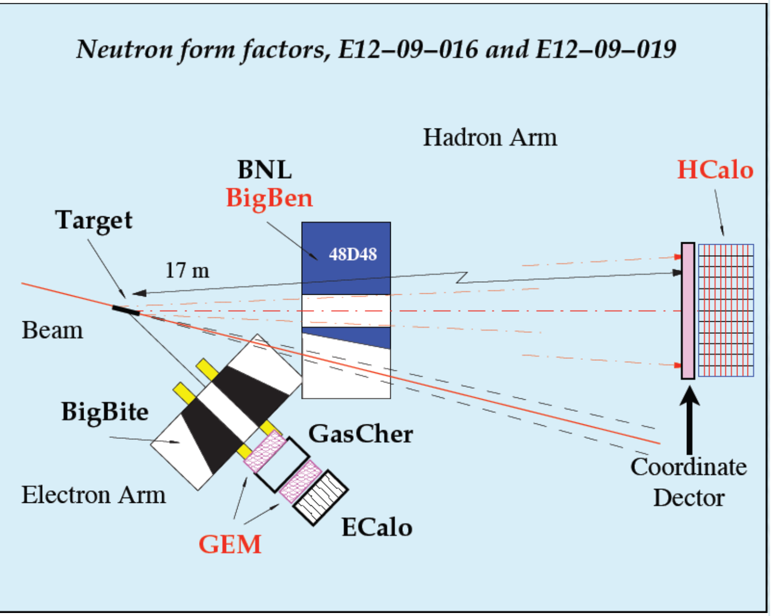

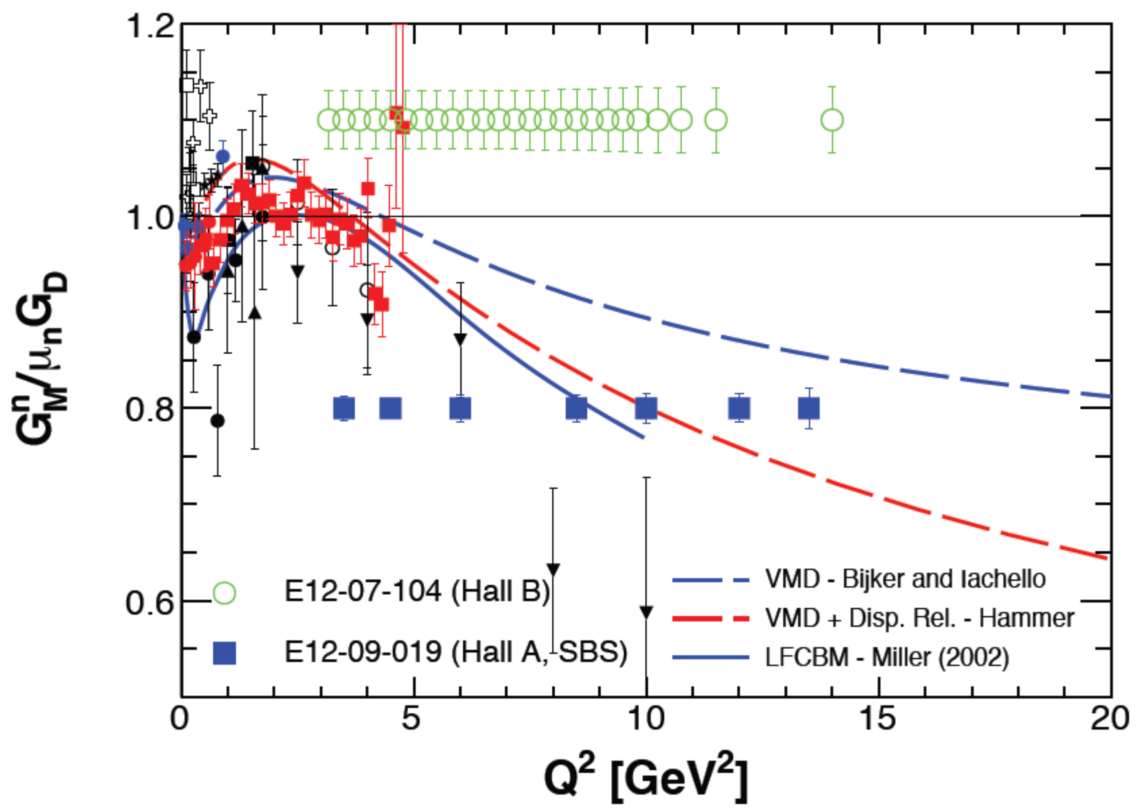

- SBS as neutron arm w/48D48 + HCAL
- Magnet sweeps charged particles out of acceptance, limiting backgrounds and "CDet" acts as charged-particle veto
- BigBite as electron arm w/upgraded 12 GeV detector package (including re-use of GEMs, built for GEP, not otherwise in use during BigBite expt's.)
- Standard LH2/LD2 target
- Different detection method—different (and smaller) systematics; complementary to CLAS12 G_{Mn} measurement
  - Overlapping collaborations between CLAS12 and SBS experiments.

Experiment E12-09-016 (G_{En} at large Q^2)

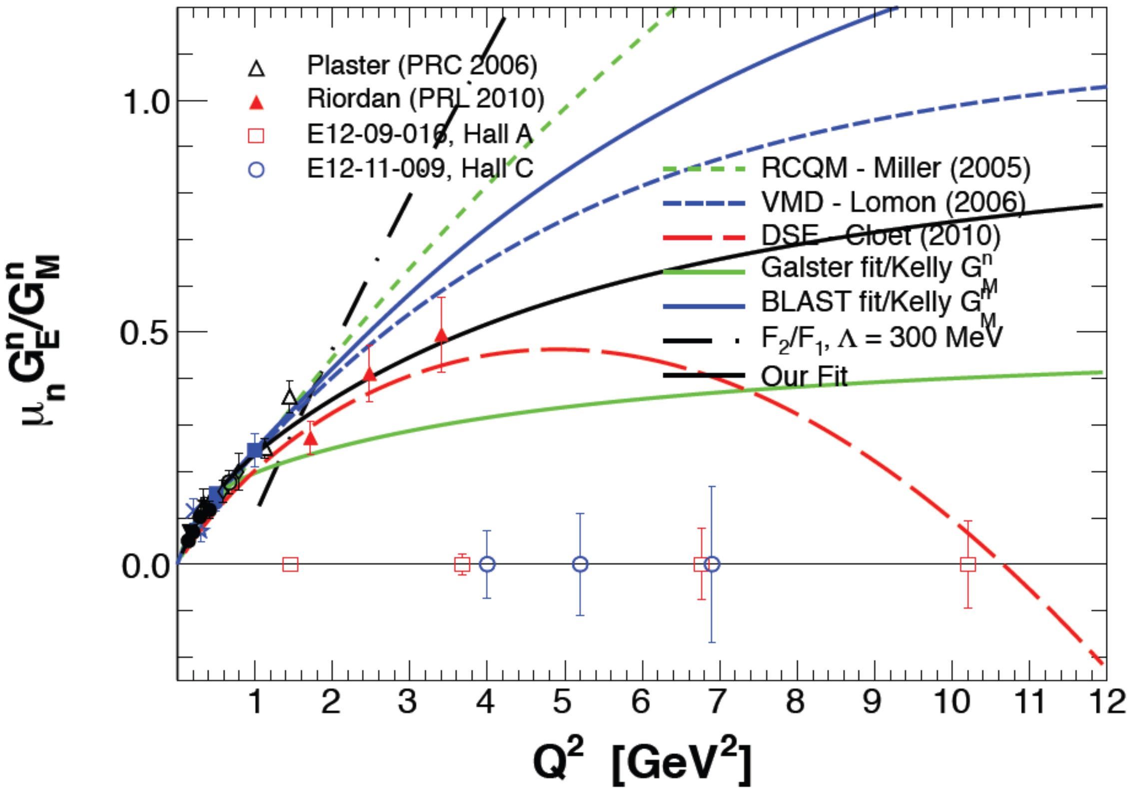

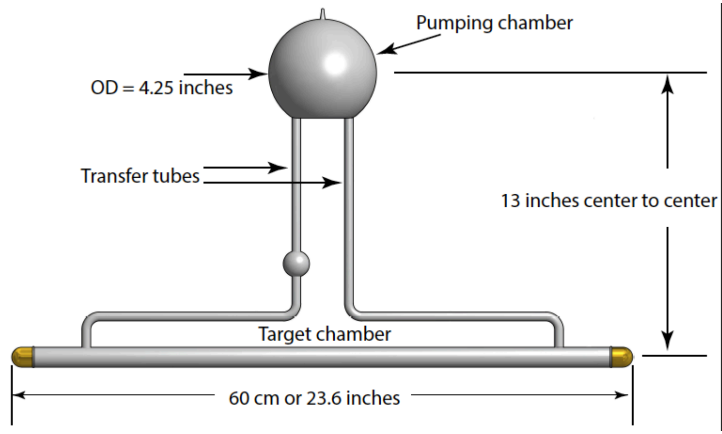

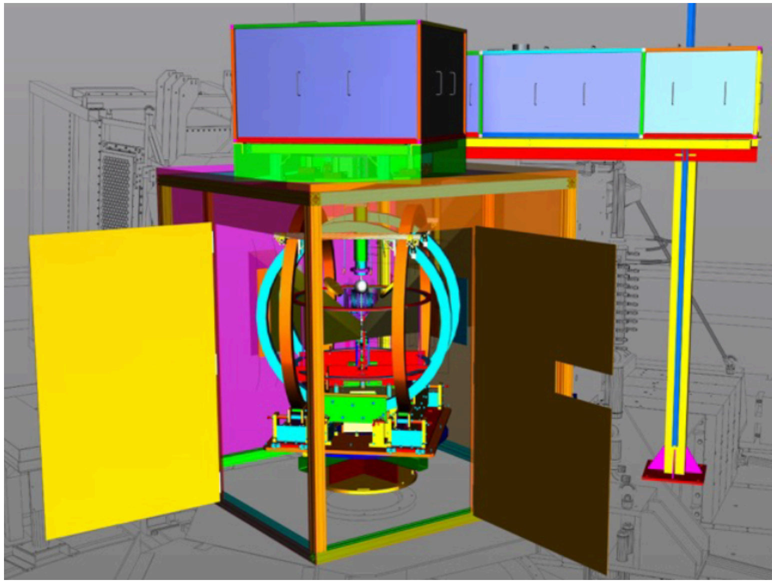

- Detector configuration same as GMN experiment
- Upgraded, high-luminosity polarized ^{3}He target based on spin-exchange optical pumping and convection-driven circulation of polarized gas between optical pumping chamber and target chamber.
- Will reach $Q^2 = 10$ GeV^2 in 50 days (approximately tripling Q^2 reach of the data)

Conceptual and Engineering Designs of Polarized ^{3}He target

The SBS Form Factor Program—Summary

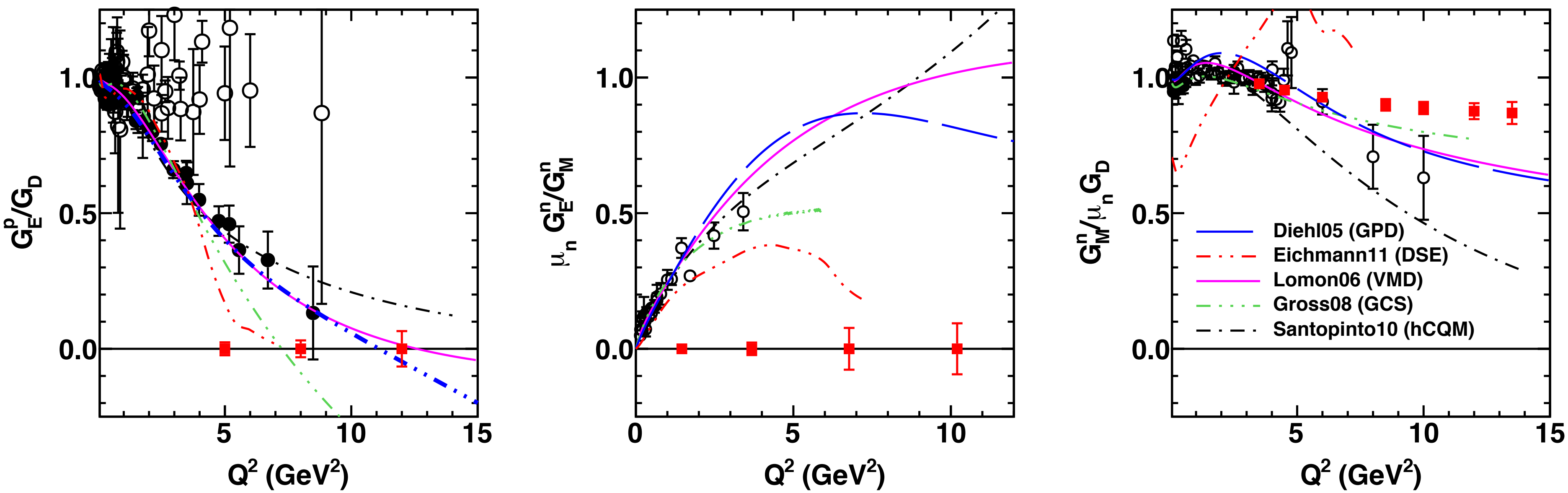

- SBS high-Q^2 form factor program:
  - Map transition to perturbative regime—running of dressed quark mass function
  - Imaging of the nucleon charge and magnetization densities in impact-parameter space in the infinite momentum frame.
  - Precision high-Q^2 form factors have significant impact on GPD extraction from DVCS
- GEP: Proton electric form factor, increase Q^2 range from 8.5 → 12 GeV^2
- GEN: Neutron electric form factor, increase Q^2 range from 3.4 → 10 GeV^2
- GMN: Neutron magnetic form factor, increase Q^2 range from 5 → 13.5 GeV^2

Summary of JLab 11 GeV high-Q^2 FF program

- The measurement of nucleon EMFFs at "large" momentum transfers Q^2 is currently a unique worldwide capability of CEBAF and one of the "flagship" science programs of the 11 GeV era.
- The high-Q^2 FFs continue to garner considerable interest from the hadronic physics theory community, given their status as (arguably) the simplest and most well-defined measurable dynamical properties of the nucleon, as a benchmark for all theoretical predictions of nucleon structure, and as an important input to the interpretation of many other experiments in nuclear and hadronic physics.
- The discrepancy between extractions of G_E^p from cross section and polarization data is still not fully understood or explained in a model-independent way.
- A coherent program of high-Q^2 FF measurements is approved that will optimally exploit the complementary capabilities of Halls A, B, and C
- The prospect of high-current, unpolarized and/or low-current, polarized e^+ beams at CEBAF would enable conclusive experimental tests of TPEX as the source of the discrepancy.

Prospects for future nucleon EMFF measurements at an EIC (JLEIC concept)

JLEIC Design Update (Apr. 2017)

energy range:

E_e: 3 to 12 GeV

E_p: 40 to 100-400 GeV

$\sqrt{s}$: 20 to 65- 140 GeV

(upper limit depends on magnet tech. choice)

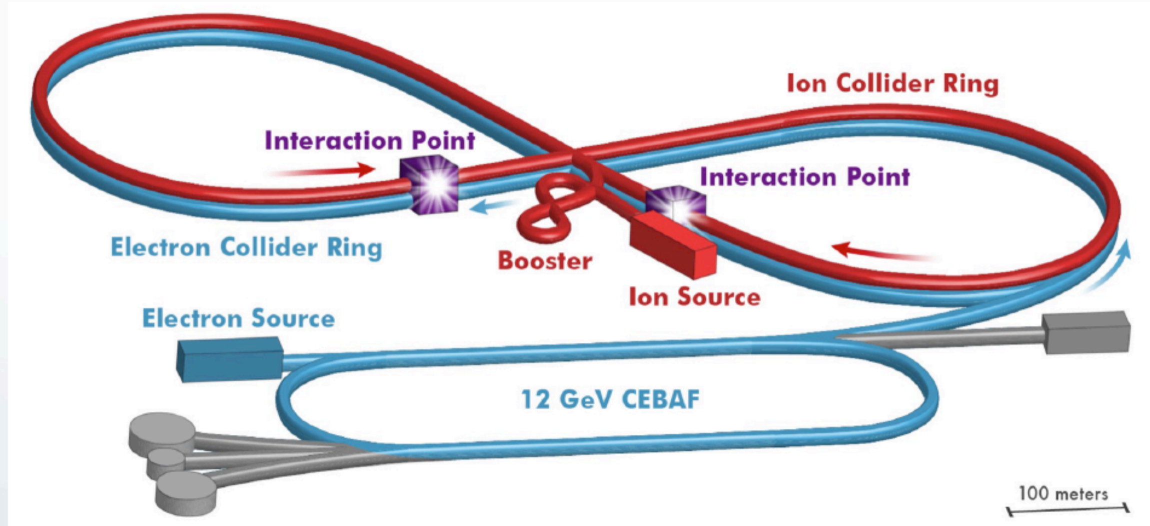

- Electron complex
  - CEBAF
  - Electron collider ring
- Ion complex
  - Ion source
  - SRF linac
  - Booster
  - Ion collider ring
- Fully integrated IR and **detector**
- DC and bunched beam **coolers**

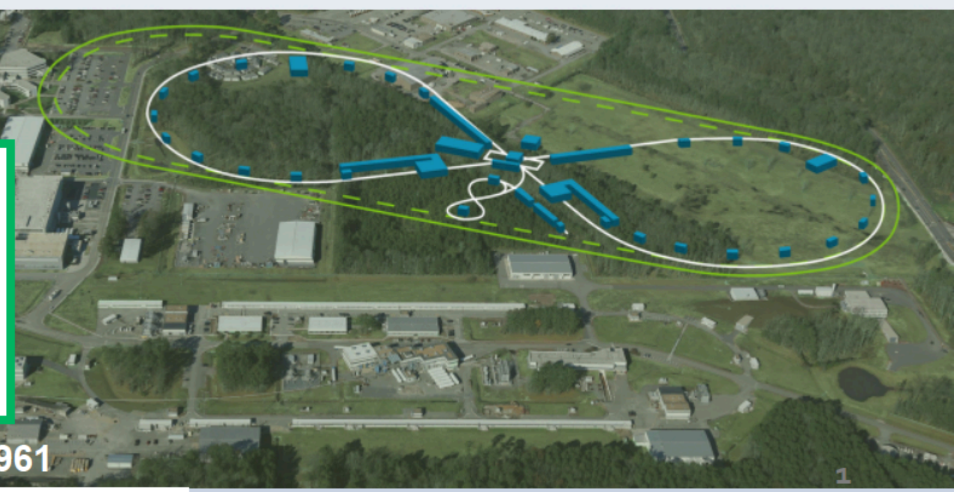

arXiv:1504.07961

April 2017 Update

JLEIC energy reach and luminosity (log)

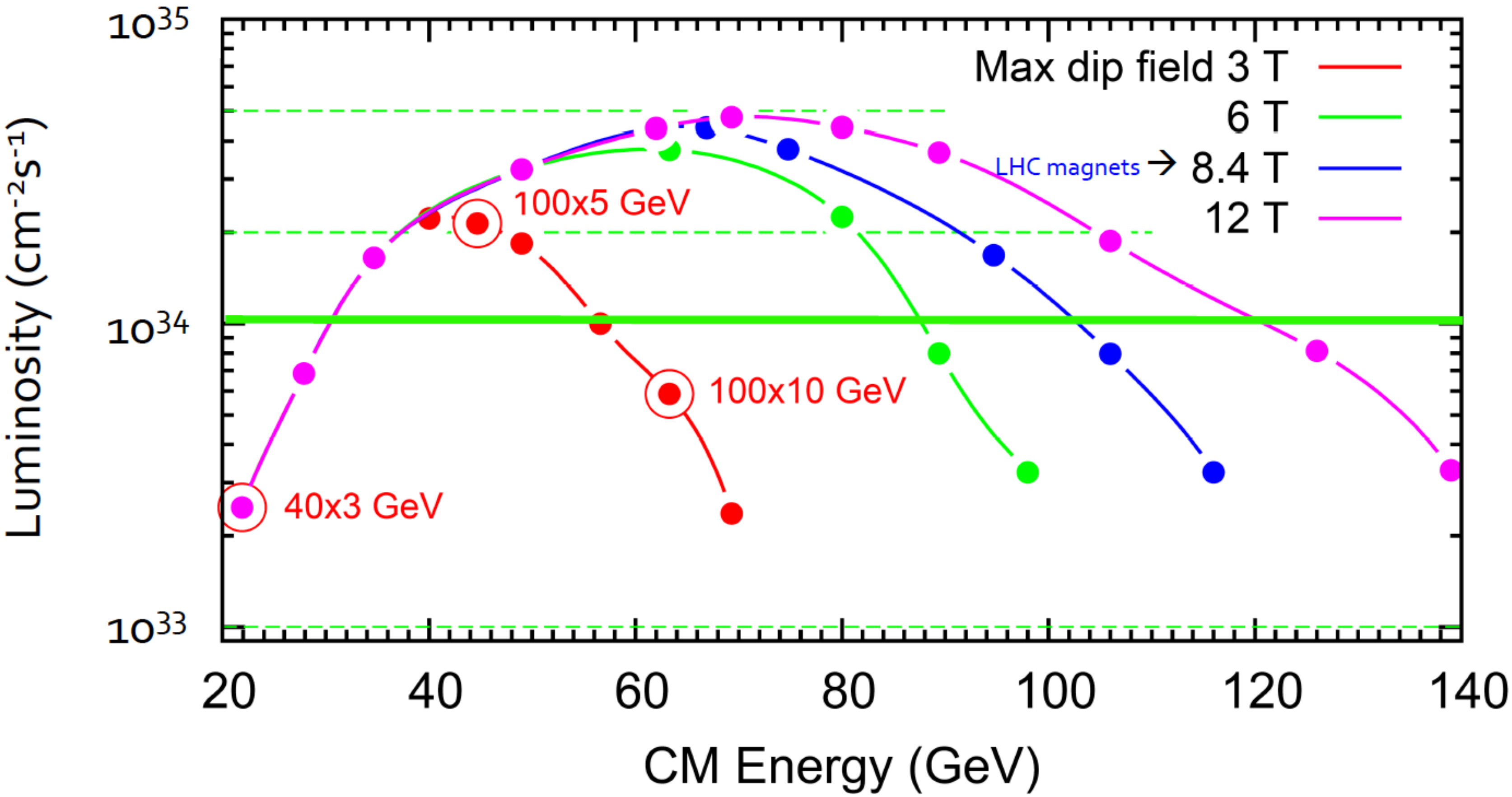

High polarization: Figure-8

- **Figure-8** concept: spin precession in one arc is exactly cancelled in the other
- **Spin stabilization by small fields**: ~3 Tm vs. ~ 400 Tm for **deuterons** at 100 GeV
  - Criterion: induced spin rotation >> spin rotation due to orbit errors
- **Polarized deuterons possible**
- **3D spin rotator**: combination of small rotations about different axes provides any polarization orientation at any point in the collider ring
- No effect on the orbit
- Adiabatic spin flips
- **Spin tracking** in progress

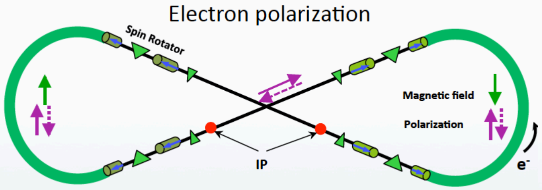

E- energy (GeV)	3	5	7	9	10
Estimated Pol. Lifetime (hours)	66	5.2	2.2	1.3	0.8

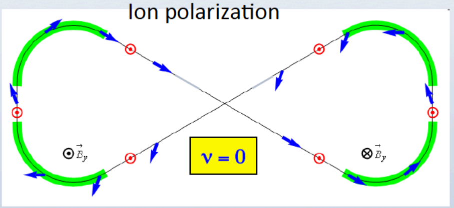

Integration IR: total acceptance

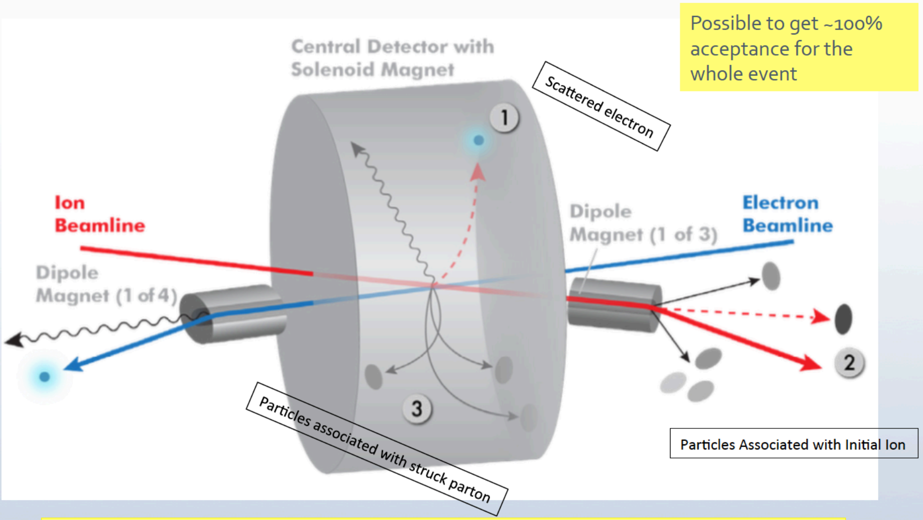

Relatively large crossing angle (**50 mr**) combined with large aperture final focus magnets, and forward dipoles are keys to this design.

High luminosity: electron cooling

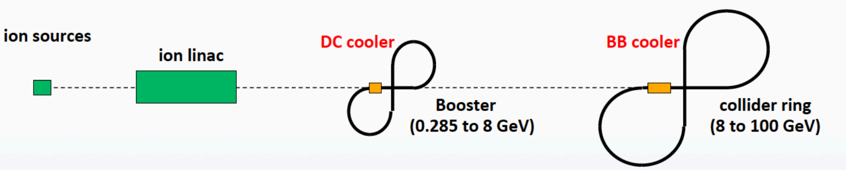

Ring	Cooler	Function	Ion energy	Electron energy
			GeV/u	MeV
Booster ring	DC	Injection and accumulation of positive ions	**0.11 ~ 0.19** (injection)	**0.062 ~ 0.1**
		Emittance reduction	**2**	**1.1**
Collider ring	Bunched Beam Cooling (BBC)	Maintain emittance during stacking	**7.9** (injection)	**4.3**
		Maintain emittance	Up to **100** (3T option)	**Up to 55**

- DC cooling for emittance reduction
- BBC cooling for emittance preservation against intra-beam scattering

JLEIC Parameters (3T option)

CM energy	GeV	21.9 (low)		44.7 (medium)		63.3 (high)	
		p	e	p	e	p	e
Beam energy	GeV	40	3	100	5	100	10
Collision frequency	MHz	476		476		476/4=119	
Particles per bunch	10^{10}	0.98	3.7	0.98	3.7	3.9	3.7
Beam current	A	0.75	2.8	0.75	2.8	0.75	0.71
Polarization	%	**80%**	**80%**	**80%**	**80%**	**80%**	**75%**
Bunch length, RMS	cm	3	1	1	1	2.2	1
Norm. emittance, hor / ver	μm	0.3/0.3	24/24	0.5/0.1	54/10.8	0.9/0.18	432/86.4
Horizontal & vertical β*	cm	8/8	13.5/13.5	6/1.2	5.1/1.0	10.5/2.1	4/0.8
Ver. beam-beam parameter		0.015	0.092	0.015	0.068	0.008	0.034
Laslett tune-shift		0.06	7×10^{-4}	0.055	6×10^{-4}	0.056	7×10^{-5}
Detector space, up/down	m	3.6/7	3.2/3	3.6/7	3.2/3	3.6/7	3.2/3
Hourglass(HG) reduction		1		0.87		0.75	
Luminosity/IP, w/HG, 10^{33}	$cm^{-2}s^{-1}$	**2.5**		**21.4**		**5.9**	

Elastic *ep* Scattering in JLEIC Kinematics (neglecting crossing angle)

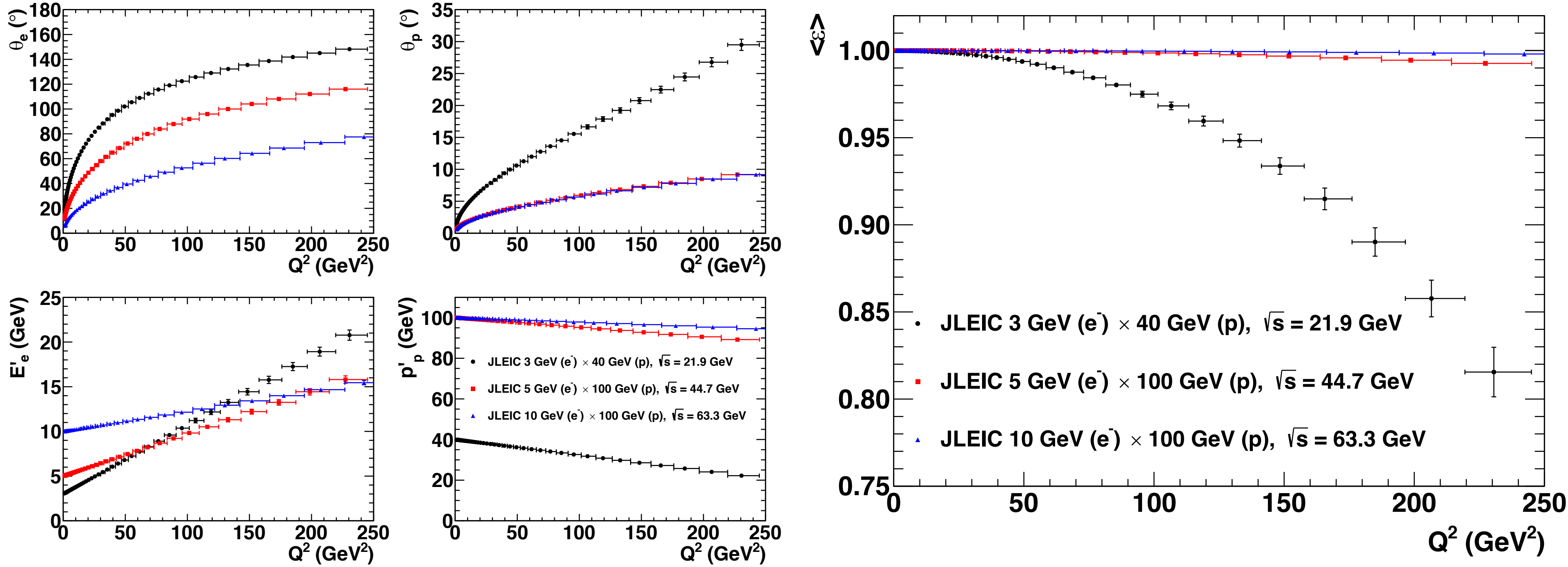

Electron and proton polar scattering angles and outgoing energies vs. Q^2, for various JLEIC energy scenarios:

- For asymmetric energy configuration ($E_p \gg E_e$), electron actually gains energy in collision (think bowling-ball ping-pong ball collision)
- Outgoing proton and electron are detectable in JLEIC "100% acceptance" IR design over a wide range of Q^2.
- Angular/momentum resolution requirements for the identification of elastic *ep* channel in the presence of dominant inelastic backgrounds needs to be evaluated
- For "reasonable" Q^2 values (unfortunately), $\epsilon \approx 1$ since $|s|, |u| \gg |t|$

$$E'_e = \frac{E_e}{1 + \frac{E_e - p_p}{E_p + p_p}\left(1 - \cos\theta_e\right)} = E_e + \frac{Q^2(p_p - E_e)}{2E_e(E_p + p_p)}$$

$$\epsilon = \frac{su - M^4}{su - M^4 + 2M^2 t - \frac{t^2}{2}}$$

Estimated elastic *ep* event rates (Born xsec.) for JLEIC scenarios

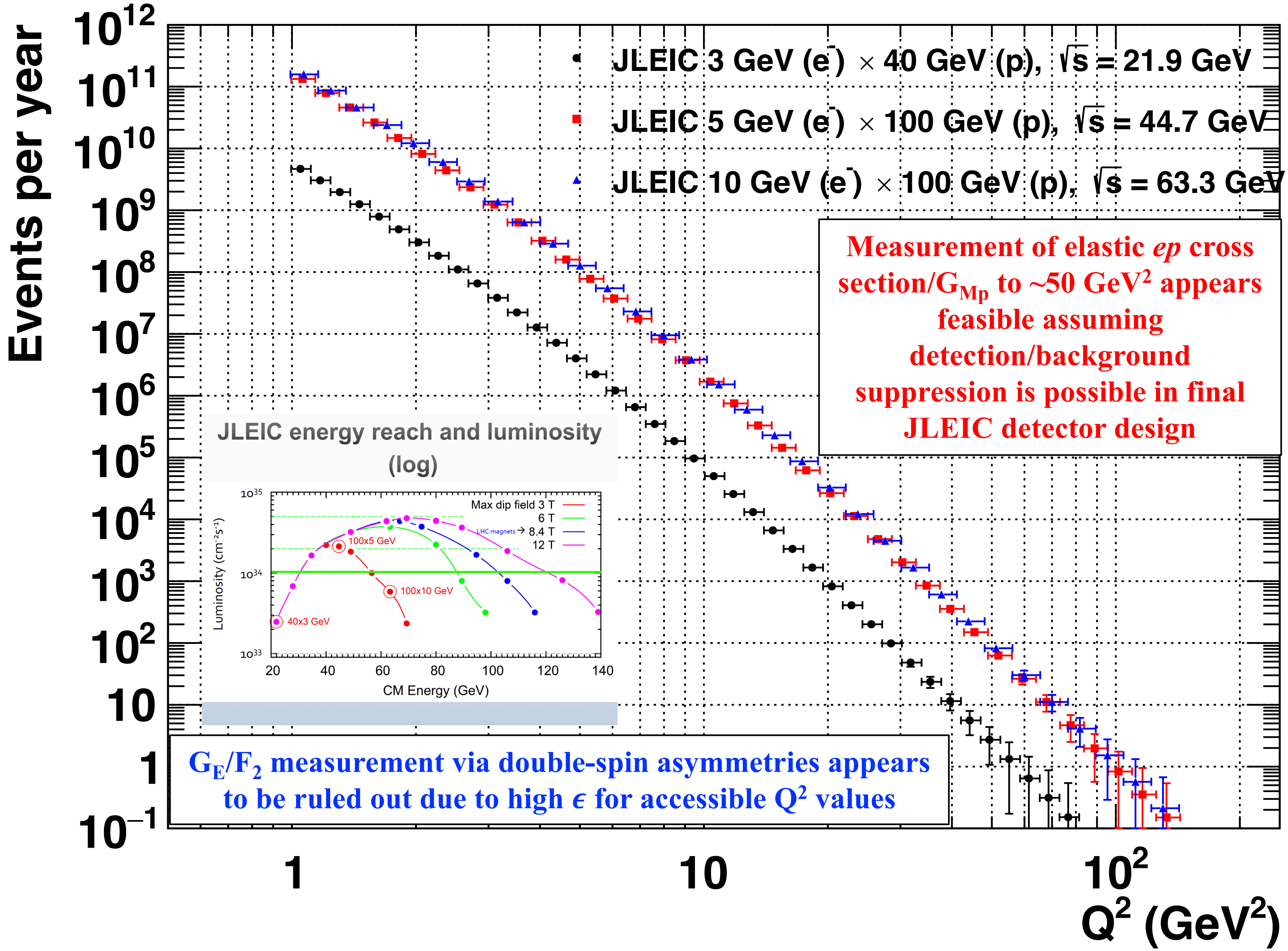

Measurement of elastic *ep* cross section/G_{Mp} to ~50 GeV^2 appears feasible assuming detection/background suppression is possible in final JLEIC detector design

G_E/F_2 measurement via double-spin asymmetries appears to be ruled out due to high ϵ for accessible Q^2 values

Theory Highlights—Why are we still interested in pushing elastic FF measurements to yet higher Q^2, when the measurements are so "hard" (in terms of cross section)?

GEp/GMp high-Q^2 polarization data are among most-cited JLab results

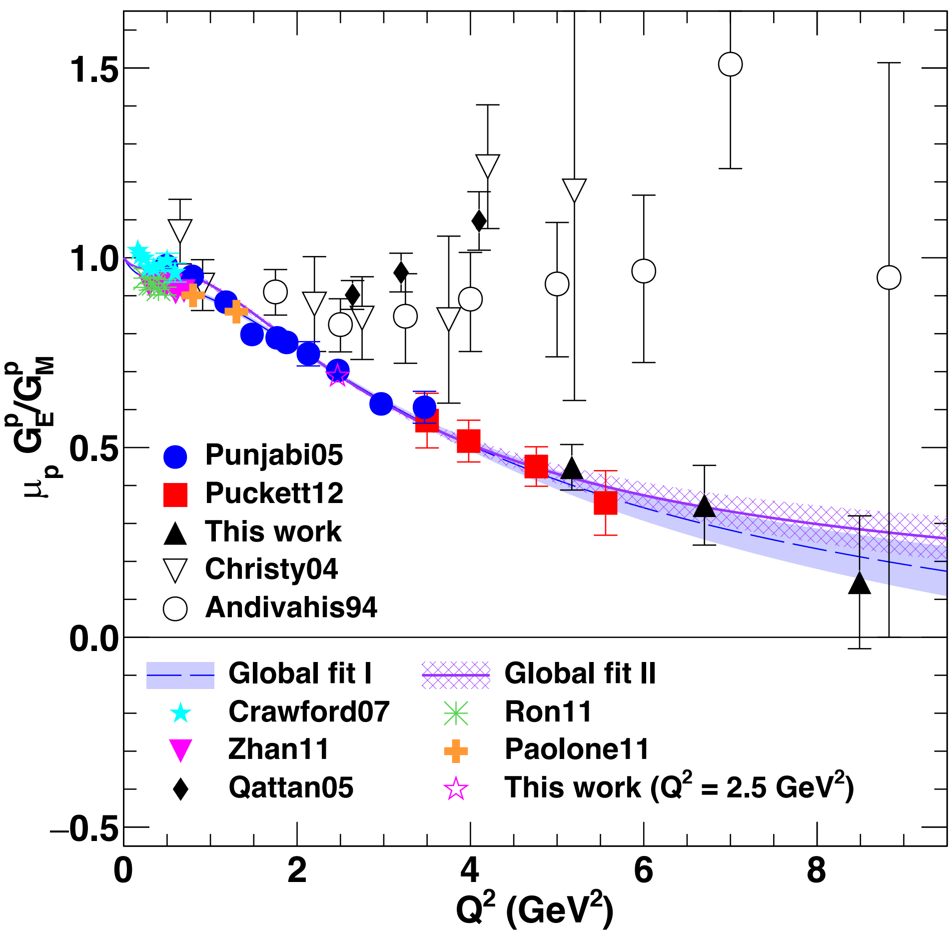

- GEp-I:
  - Jones *et al.*, **Phys. Rev. Lett. 84 (2000) 1398-1402: 843 INSPIRE-HEP citations**
  - Punjabi *et al.*, **Phys.Rev. C71 (2005) 055202: 410 INSPIRE-HEP citations**
- GEp-II:
  - Gayou *et al.*, **Phys.Rev.Lett. 88 (2002) 092301: 766 INSPIRE-HEP citations**
  - Puckett *et al.*, **Phys.Rev. C85 (2012) 045203: 126 INSPIRE-HEP citations**
- GEp-III/GEp-2γ:
  - Puckett *et al.*, **Phys.Rev.Lett. 104 (2010) 242301,** 238 INSPIRE-HEP citations
  - Meziane *et al.*, **Phys.Rev.Lett. 106 (2011) 132501,** 72 INSPIRE-HEP citations
  - Puckett *et al.*, **Phys.Rev. C96 (2017) no.5, 055203,** 8 INSPIRE-HEP citations
- Low-Q^2 data from JLab:
  - Ron *et al.*, **Phys.Rev.Lett. 99 (2007) 202002**, 68 INSPIRE-HEP citations
  - Ron *et al.*, **Phys.Rev. C84 (2011) 055204,** 87 INSPIRE-HEP citations
  - Zhan *et al.*, **Phys.Lett. B705 (2011) 59-64,** 152 INSPIRE-HEP citations
  - Paolone *et al.*, **Phys.Rev.Lett. 105 (2010) 072001**, 80 INSPIRE-HEP citations

Doug Higinbotham's listing of "Hall A" publications by citation count:

CIPANP 2018 - Thirteenth Con × | CIPANP 2018 - Thirteenth Con × | Experimental Hall A ×

hallaweb.jlab.org/publications/

Apps | Bookmarks | Bookmarks | Imported From Fire... | Student evaluation... | dis 2018 kobe japa... | Promotion, Tenure,... | 0 Notifications

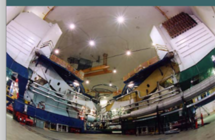

Publication Lists

- DOI Numbers

Jefferson Lab Database

- Home
- Thesis List
- Search
- Submit

Internal Documents

- Annual Reports (current) | (archive)
- Technical Notes

Publication Archives

- arXiv.org
- inspire

Total of 113 Hall A Refereed Publications
compiled Tue Feb 27 06:50:08 EST 2018

Renowned Papers (500+ inspire citations)

Gayou *et al.*, Phys. Rev. Lett., **88** (2002) 092301. (arXiv) | (doi) | (inspire) | (pdf)
Jones *et al.*, Phys. Rev. Lett., **84** (2000) 1398-1402. (arXiv) | (doi) | (inspire) | (pdf)

Famous Papers (250-499 inspire citations)

Qattan *et al.*, Phys. Rev. Lett., **94** (2005) 142301. (arXiv) | (doi) | (inspire) | (pdf)
Punjabi *et al.*, Phys. Rev., **C71** (2005) 055202. (arXiv) | (doi) | (inspire) | (pdf)

Very Well-Known Paper (100-249 inspire citations)

Abrahamyan *et al.*, Phys. Rev. Lett., **108** (2012) 112502. (arXiv) | (doi) | (inspire) | (pdf)
Abrahamyan *et al.*, Phys. Rev. Lett., **107** (2011) 191804. (arXiv) | (doi) | (inspire) | (pdf)
Qian *et al.*, Phys. Rev. Lett., **107** (2011) 072003. (arXiv) | (doi) | (inspire) | (pdf)
Puckett *et al.*, Phys. Rev., **C85** (2012) 045203. (arXiv) | (doi) | (inspire) | (pdf)
Zhan *et al.*, Phys. Lett., **B705** (2011) 59-64. (arXiv) | (doi) | (inspire) | (pdf)
Weinstein *et al.*, Phys. Rev. Lett., **106** (2011) 052301. (arXiv) | (doi) | (inspire) | (pdf)
Riordan *et al.*, Phys. Rev. Lett., **105** (2010) 262302. (arXiv) | (doi) | (inspire) | (pdf)
Puckett *et al.*, Phys. Rev. Lett., **104** (2010) 242301. (arXiv) | (doi) | (inspire) | (pdf)
Subedi *et al.*, Science, **320** (2008) 1476-1478. (arXiv) | (doi) | (inspire) | (pdf)
Mazouz *et al.*, Phys. Rev. Lett., **99** (2007) 242501. (arXiv) | (doi) | (inspire) | (pdf)
Shneor *et al.*, Phys. Rev. Lett., **99** (2007) 072501. (arXiv) | (doi) | (inspire) | (pdf)
Acha *et al.*, Phys. Rev. Lett., **98** (2007) 032301. (arXiv) | (doi) | (inspire) | (pdf)
Camacho *et al.*, Phys. Rev. Lett., **97** (2006) 262002. (arXiv) | (doi) | (inspire) | (pdf)
Aniol *et al.*, Phys. Lett., **B635** (2006) 275-279. (arXiv) | (doi) | (inspire) | (pdf)
Aniol *et al.*, Phys. Rev. Lett., **96** (2006) 022003. (arXiv) | (doi) | (inspire) | (pdf)
Amarian *et al.*, Phys. Rev. Lett., **92** (2004) 022301. (arXiv) | (doi) | (inspire) | (pdf)
Alcorn *et al.*, Nucl. Instrum. Meth., **A522** (2004) 294-346. (doi) | (inspire)
Zheng *et al.*, Phys. Rev., **C70** (2004) 065207. (arXiv) | (doi) | (inspire) | (pdf)
Aniol *et al.*, Phys. Rev., **C69** (2004) 065501. (arXiv) | (doi) | (inspire) | (pdf)
Zheng *et al.*, Phys. Rev. Lett., **92** (2004) 012004. (arXiv) | (doi) | (inspire) | (pdf)
Strauch *et al.*, Phys. Rev. Lett., **91** (2003) 052301. (arXiv) | (doi) | (inspire) | (pdf)
Amarian *et al.*, Phys. Rev. Lett., **89** (2002) 242301. (arXiv) | (doi) | (inspire) | (pdf)
Aniol *et al.*, Phys. Lett., **B635** (2006) 275-279. (arXiv) | (doi) | (inspire) | (pdf)
Xu *et al.*, Phys. Rev. Lett., **85** (2000) 2900-2904. (arXiv) | (doi) | (inspire) | (pdf)
Aniol *et al.*, Phys. Rev. Lett., **82** (1999) 1096-1100. (arXiv) | (doi) | (inspire) | (pdf)

Well-known Papers (50-99 inspire citations)

Hen *et al.*, Science, **346** (2014) 614-617. (arXiv) | (doi) | (inspire) | (pdf)
Ahmed *et al.*, Phys. Rev. Lett., **108** (2012) 102001. (arXiv) | (doi) | (inspire) | (pdf)
Huang *et al.*, Phys. Rev. Lett., **108** (2012) 052001. (arXiv) | (doi) | (inspire) | (pdf)
Arrington *et al.*, Prog. Part. Nucl. Phys., **67** (2012) 898-938. (arXiv) | (doi) | (inspire) | (pdf)
Ron *et al.*, Phys. Rev., **C84** (2011) 055204. (arXiv) | (doi) | (inspire) | (pdf)
Meziane *et al.*, Phys. Rev. Lett., **106** (2011) 132501. (arXiv) | (doi) | (inspire) | (pdf)
Paolone *et al.*, Phys. Rev. Lett., **105** (2010) 072001. (arXiv) | (doi) | (inspire) | (pdf)

Papers directly related to Elastic nucleon EMFFs

High-Q² Nucleon Form Factors, GPDs and Spin

Flavor decomposition of nucleon EMFFs (neglecting strangeness):

$$F^p_{1,2} \approx e_u F^u_{1,2} + e_d F^d_{1,2}$$

$$F^n_{1,2} \approx e_u F^d_{1,2} + e_d F^u_{1,2}$$

Quark flavor FFs are integrals of valence quark GPDs H and E at zero skewness :

$$F_1^q(t) = \int_0^1 H_v^q(x,t)dx$$

$$F_2^q(t) = \int_0^1 E_v^q(x,t)dx$$

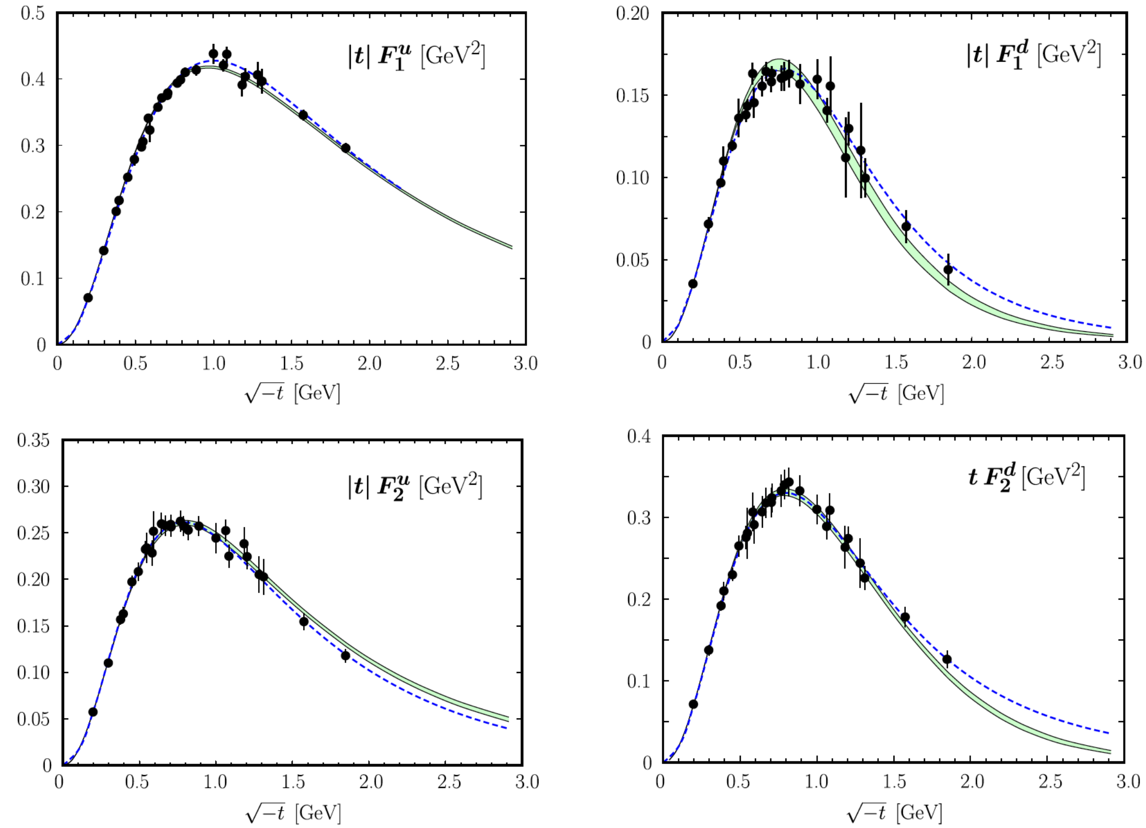

Phys.Rev.Lett. 78 (1997) 610-613: Ji sum rule for total angular momentum

$$J_q = \frac{1}{2}\int_{-1}^{+1} dx x[H^q(x,\xi,t=0) + E^q(x,\xi,t=0)].$$

Diehl, Kroll. Eur. Phys. J. C (2013) 73:2397

- FF data + forward PDFs from global DIS fits → model-dependent extraction of GPDs
- Compute valence-quark contributions to the Ji sum rule: $J_v^u = 0.230^{+0.009}_{-0.024}, \quad J_v^d = -0.004^{+0.010}_{-0.016}$

The under-appreciated importance of knowledge of the high-Q^2 FFs in the extraction of GPDs from experiment

From the recent paper by **M. Diehl and P. Kroll. Eur. Phys. J. C (2013) 73:2397**

- "This requires an ansatz for the functional form of the GPDs and in this sense is intrinsically model dependent, but on the other hand it can reach values of the invariant momentum transfer t much larger than what can conceivably be measured in hard exclusive scattering..."
- "We note that the electromagnetic form factors provide indirect constraints on GPDs at high values of t, which will conceivably never be accessible in hard exclusive scattering processes."

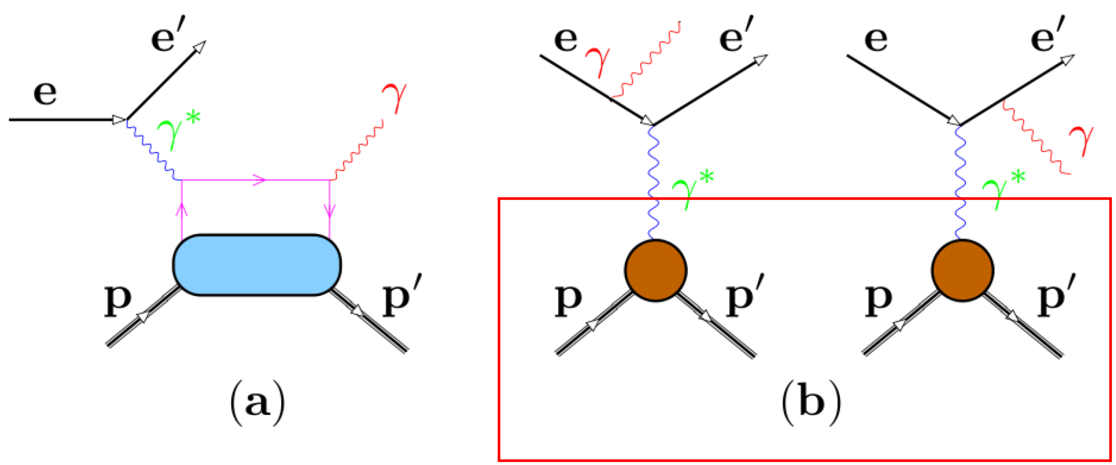

- DVCS experiments actually measure the interference of Bethe-Heitler and DVCS handbag mechanism at the same order of $\alpha \rightarrow$ precise knowledge of elastic FFs over a wide range of Q^2 is needed to separate DVCS contribution!
- EMFFs thus provide both direct constraints to GPDs via the sum rules and crucial input to the extraction of Compton Form Factors from experimental observables

Exposing the dressed-quark mass function

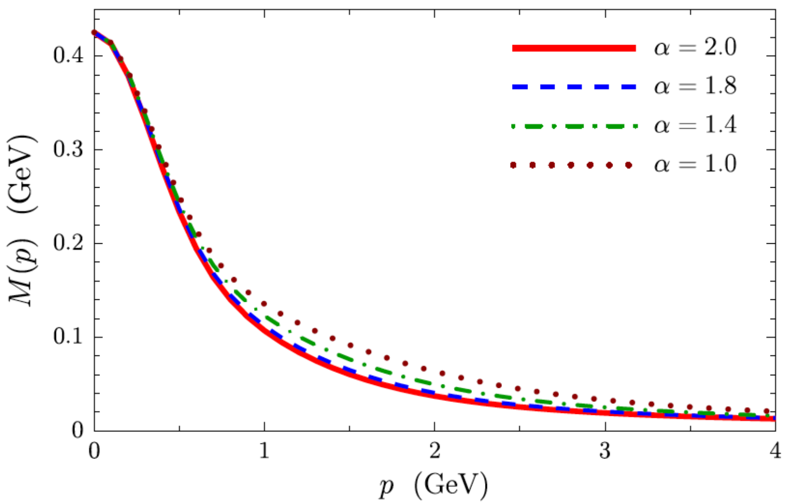

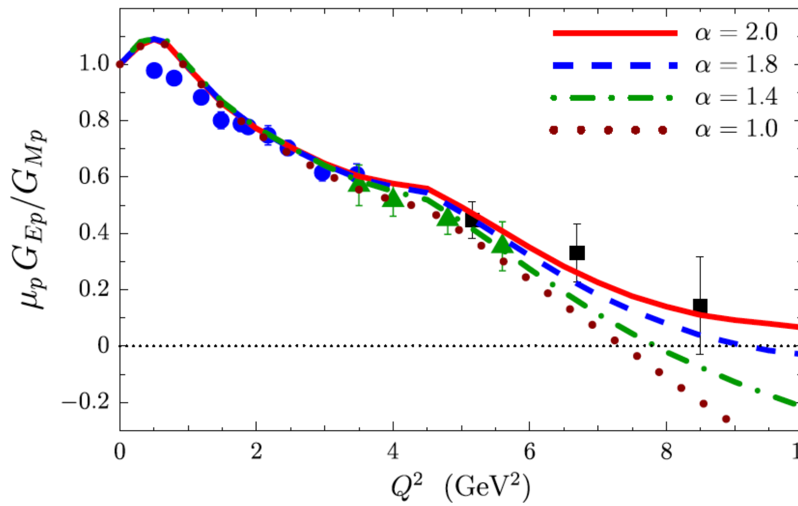

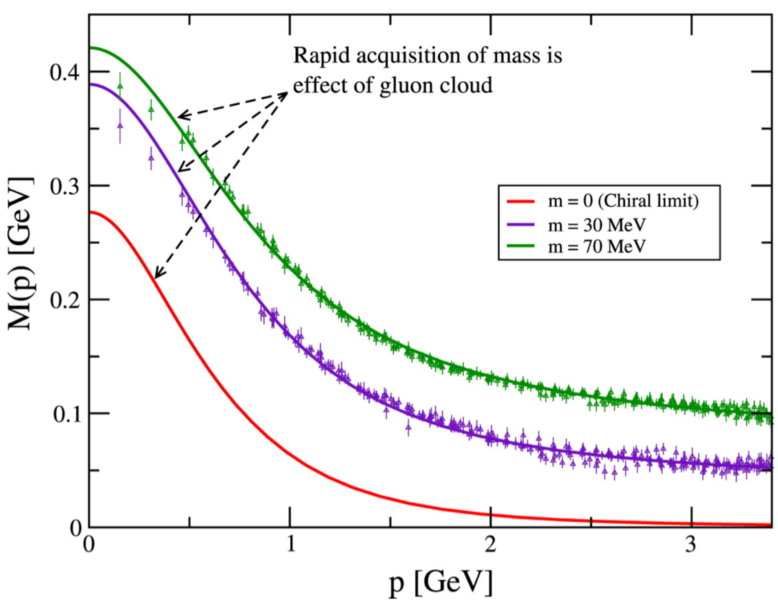

In the framework of Dyson-Schwinger equations, the high-Q^2 nucleon FFs ($Q^2 > 5$ GeV^2) are especially sensitive to momentum-dependent dressed-quark mass function in the few-GeV region, see e.g.,:

- I. Cloet, C. Roberts, A. Thomas: “Revealing Dressed Quarks via the Proton’s Charge Distribution”, **PRL 111, 101803 (2013)**
- I. Cloet and C. Roberts: “Explanation and Prediction of Observables Using Continuum Strong QCD”, arxiv:1310.2651v2 (2013), **PPNP 77 (2014), 1-69**

Dyson-Schwinger Equations, diquark correlations, and zero crossings of G_{Ep}, G_{En}

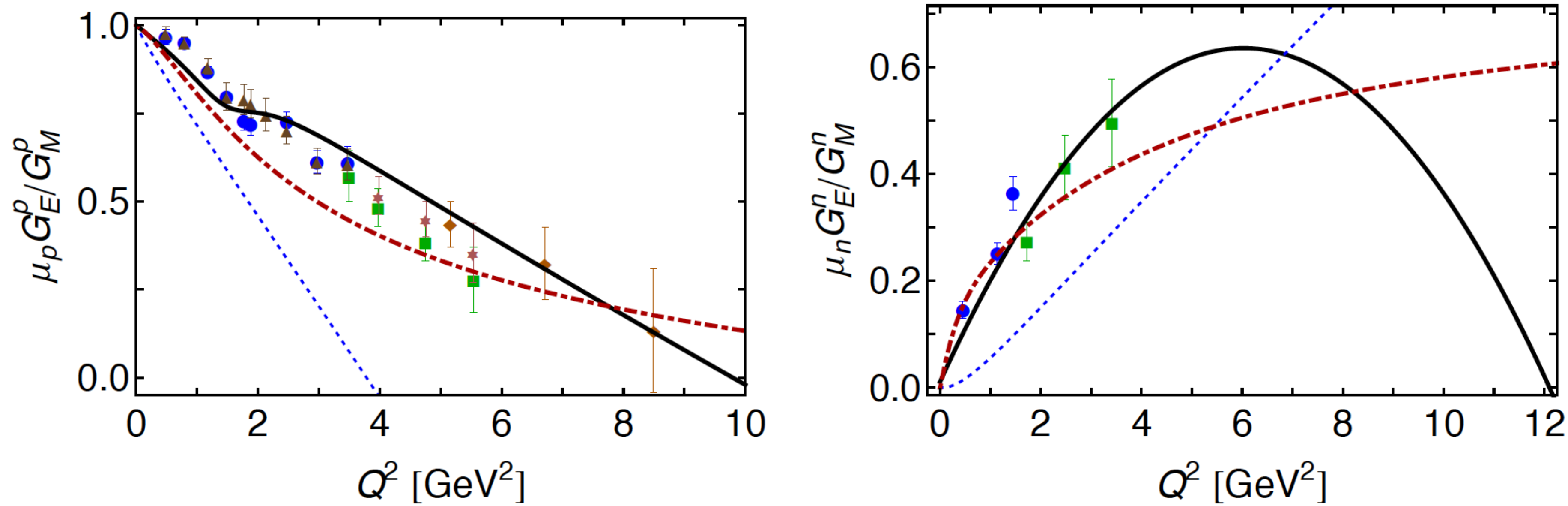

Fig. 3 *Left panel*: normalised ratio of proton electric and magnetic form factors. Curves: *solid, black* – result obtained herein, using our QCD-kindred framework; *Dashed, blue* – CI result [18]; and *dot-dashed, red* – ratio inferred from 2004 parametrisation of experimental data [65]. Data: blue circles [68]; green squares [69]; brown triangles [70]; purple asterisk [71]; and orange diamonds [72]. *Right panel*: normalised ratio of neutron electric and magnetic form factors. Curves: same as in left panel. Data: blue circles [73]; and green squares [74].

J. Segovia, I. Cloet and C. Roberts: Few-Body Syst. 55, 1185 (2014)

Quote from the abstract:

of dynamical chiral symmetry breaking in the bound-state problem. Amongst the results we describe, the following are of particular interest: $G_E^p(Q^2)/G_M^p(Q^2)$ possesses a zero at $Q^2 = 9.5\,\mathrm{GeV}^2$; any change in the interaction which shifts a zero in the proton ratio to larger Q^2 relocates a zero in $G_E^n(Q^2)/G_M^n(Q^2)$ to smaller Q^2; there is likely a value of momentum transfer above which $G_E^n > G_E^p$; and the presence of strong diquark correlations within the nucleon is sufficient to understand empirical extractions of the flavour-separated form factors. Regarding the $\Delta(1232)$-baryon, we find that, *inter*

Reaching high Q^2 in Lattice QCD

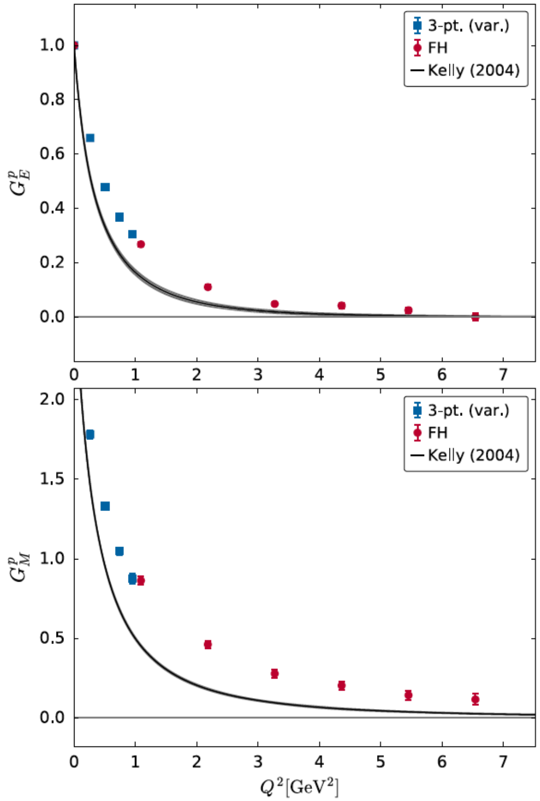

FIG. 3. G_E and G_M for the proton from the Feynman-Hellmann method and from a variational method described in Ref. [29] employed on the same ensemble. The experimental parametrization is from Ref. [49].

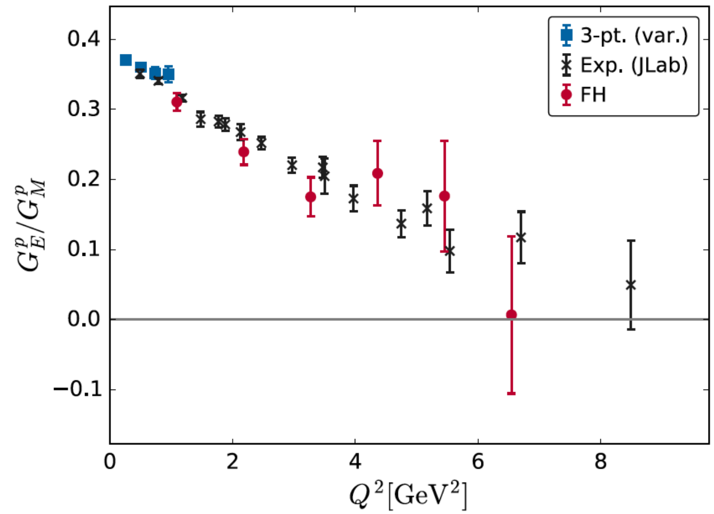

FIG. 4. Ratio G_E/G_M for the proton from the application of the Feynman-Hellmann method, from a variational analysis of three-point functions [29], and from experiment [5–7]. Note this is not scaled by the magnetic moment of the proton μ_p, as this would require phenomenological fits to the low-Q^2 data, which is not the focus of this work.

$$\frac{\partial E_\psi}{\partial \lambda} = \left\langle \psi \left| \frac{\partial H}{\partial \lambda} \right| \psi \right\rangle$$

A. J. Chambers *et al.*, (QCDSF/UKQCD/CSSM Collaborations) Phys. Rev. D 96, 114509 (2017)

- Novel application of the Feynman-Hellman method: relates hadronic matrix elements to energy shifts, allowing access to form factors via two-point correlators as opposed to more complicated three-point functions; improves signal-to-noise ratio for high-momentum states

Transition to pQCD–onset of dimensional scaling?

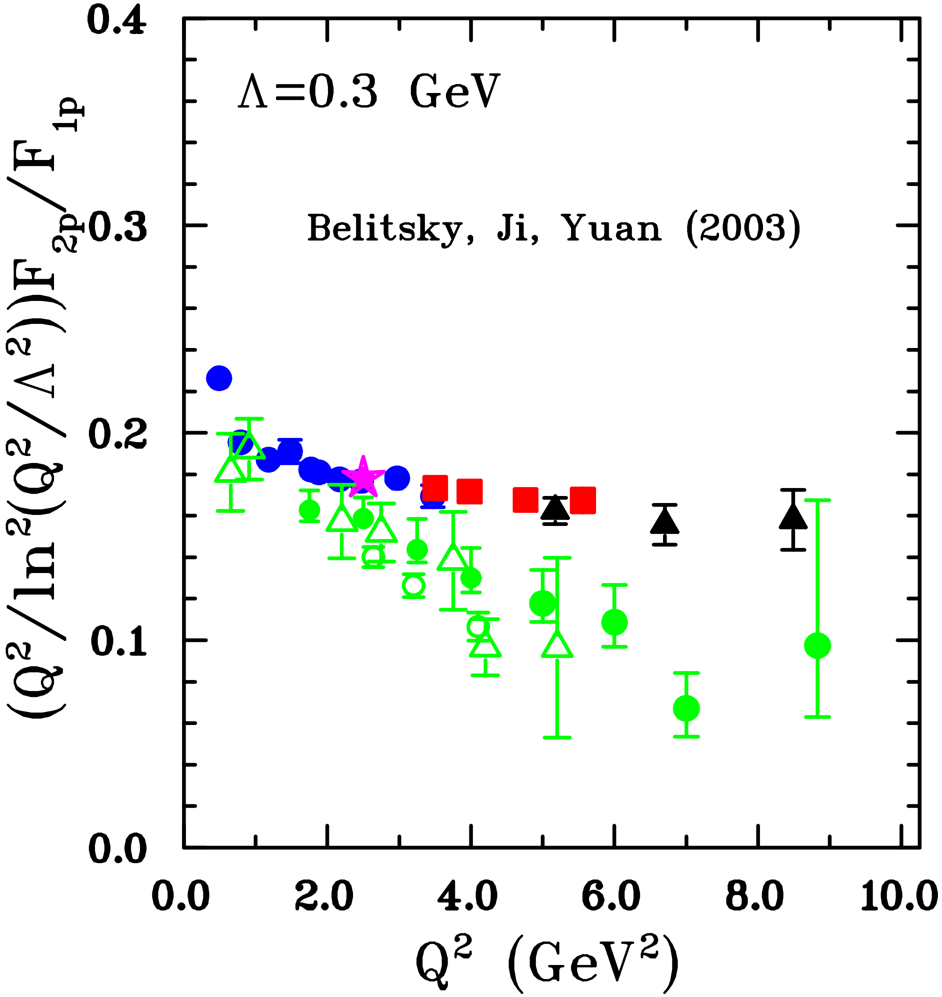

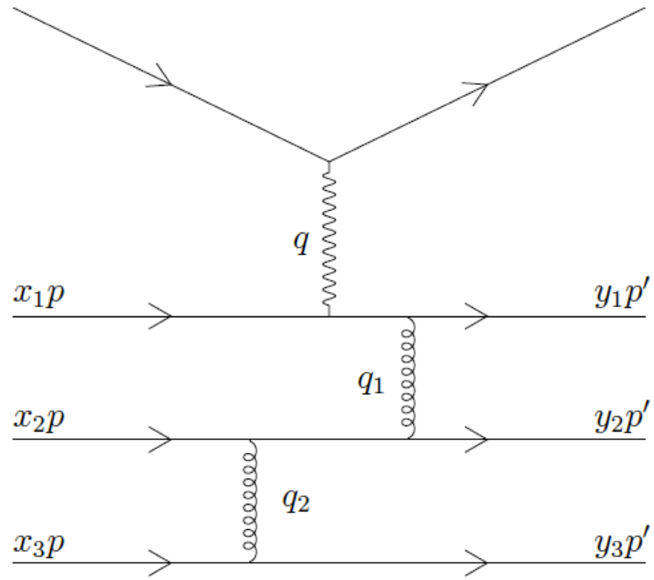

- Brodsky, Farrar, PRD 11, 1309 (1975) $F_1 \propto \frac{\alpha_S^2}{Q^4}$
- Brodsky, Lepage PRL 43, 545 (1979) $F_2 \propto \frac{F_1}{Q^2}$
- Belitsky, Ji, Yuan, PRL 91, 092003 (2003) $\left(\frac{Q^2}{\ln^2\left(\frac{Q^2}{\Lambda^2}\right)}\right) F_2^p \propto F_1^p$

"Precocious" scaling observed in F_2^p/F_1^p not seen in F_2^n/F_1^n, for values of cutoff parameter Λ similar to that which describes proton data

Rosenbluth-Polarization Discrepancy and Two-Photon-Exchange

- "Standard" QED radiative corrections to ep cross section data at lowest order in α include:
  - Vertex corrections
  - Vacuum polarization
  - Self-energy
  - Bremsstrahlung
- Two-photon exchange (TPEX) process where both photons are "hard": previously neglected
  - **Cannot be calculated model-independently**
  - **Has been shown to partially resolve the discrepancy between L/T and polarization data for G_{Ep}**

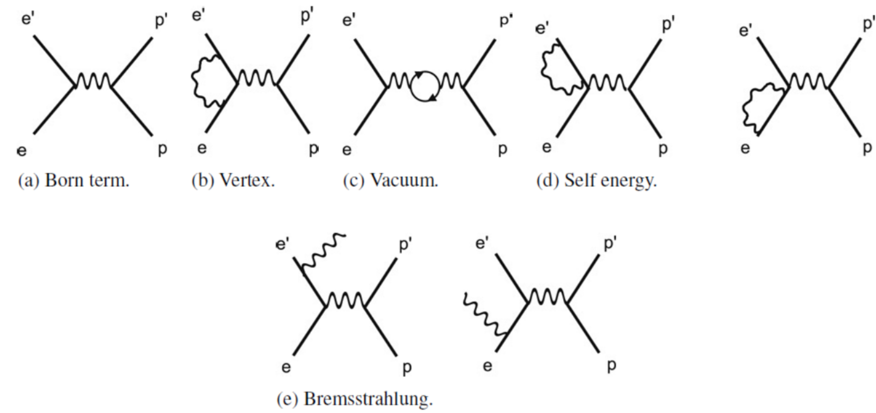

Fig. 24. Born term and lowest order radiative correction graphs for the electron in elastic *ep*.

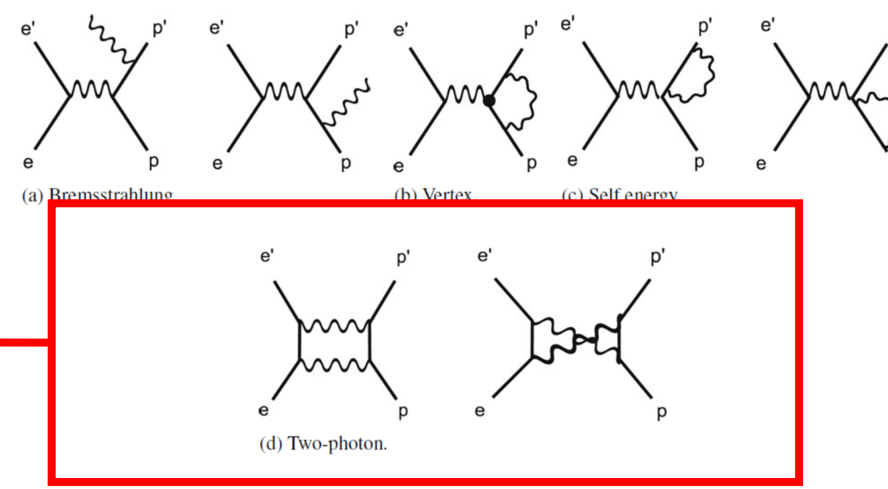

Status of TPEX

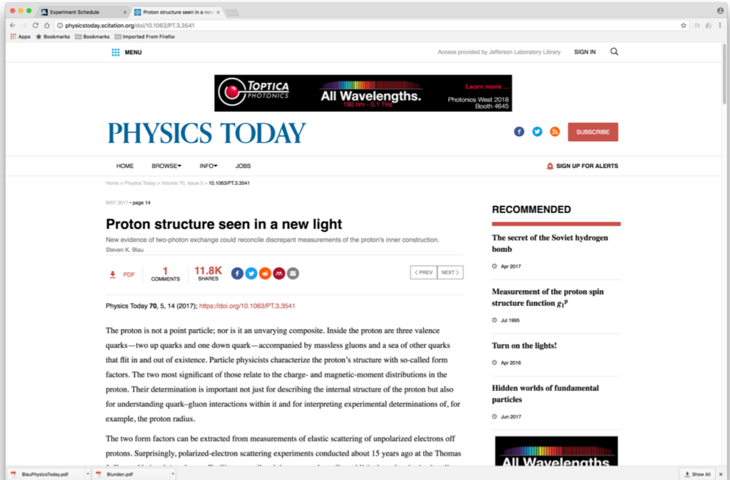

PHYSICS TODAY

HOME BROWSE INFO JOBS

Home > Physics Today > Volume 70, Issue 5 > 10.1063/PT.3.3541

MAY 2017 • page 14

Proton structure seen in a new light

New evidence of two-photon exchange could reconcile discrepant measurements of the proton's inner construction.

Steven K. Blau

PDF 1 COMMENTS 11.8K SHARES

Physics Today 70, 5, 14 (2017); https://doi.org/10.1063/PT.3.3541

The proton is not a point particle; nor is it an unvarying composite. Inside the proton are three valence quarks—two up quarks and one down quark—accompanied by massless gluons and a sea of other quarks that flit in and out of existence. Particle physicists characterize the proton's structure with so-called form factors. The two most significant of those relate to the charge- and magnetic-moment distributions in the proton. Their determination is important not just for describing the internal structure of the proton but also for understanding quark–gluon interactions within it and for interpreting experimental determinations of, for example, the proton radius.

The two form factors can be extracted from measurements of elastic scattering of unpolarized electrons off protons. Surprisingly, polarized-electron scattering experiments conducted about 15 years ago at the Thomas

RECOMMENDED

The secret of the Soviet hydrogen bomb

Measurement of the proton spin structure function g_1^p

Turn on the lights!

Hidden worlds of fundamental particles

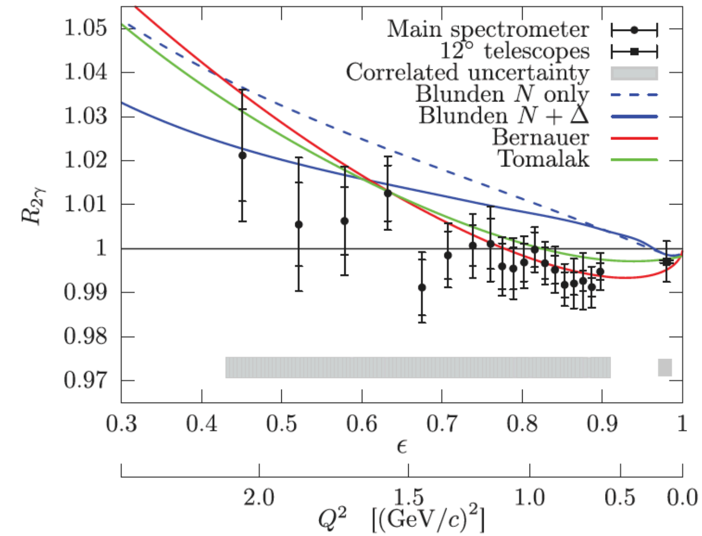

FIG. 2. OLYMPUS result for $R_{2\gamma}$ using the Mo-Tsai [21] prescription for radiative corrections to all orders. Uncertainties shown are statistical (inner bars), uncorrelated systematic (added in quadrature, outer bars), and correlated systematic (gray band). Note the 12° data point at $\epsilon = 0.978$ is completely dominated by systematic uncertainties.

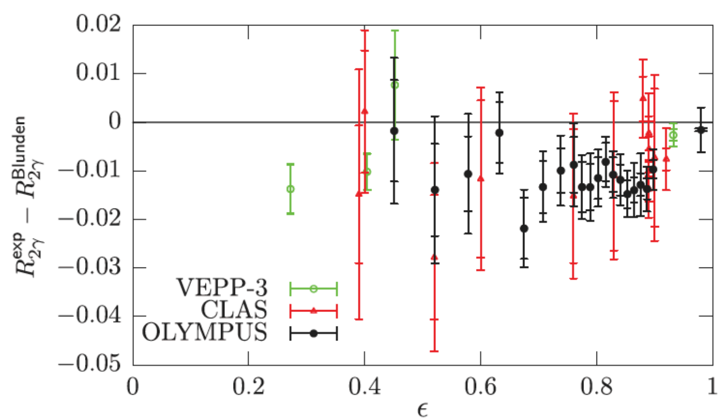

FIG. 3. Comparison of the recent results to the calculation by Blunden. The data are in good agreement, but generally fall below the prediction. Please note that data at similar ϵ values have been measured at different Q^2. Also note that the VEPP-3 data have been normalized to the calculation at high ϵ.

- Henderson *et al.*, (OLYMPUS Collaboration): Phys. Rev. Lett. 118, 092501 (2017)
- S. K. Blau, Physics Today 70, 14 (2017)
- Blunden TPEX calculation with N and N+Δ intermediate states is consistent with recent e+p/e-p cross section ratios from CLAS-TPE, VEPP-3 (Novosibirsk), and OLYMPUS data.
- However, all of these data have $Q^2 \leq 2.1$ GeV^2

Backups

Nucleon FFs and GPDs

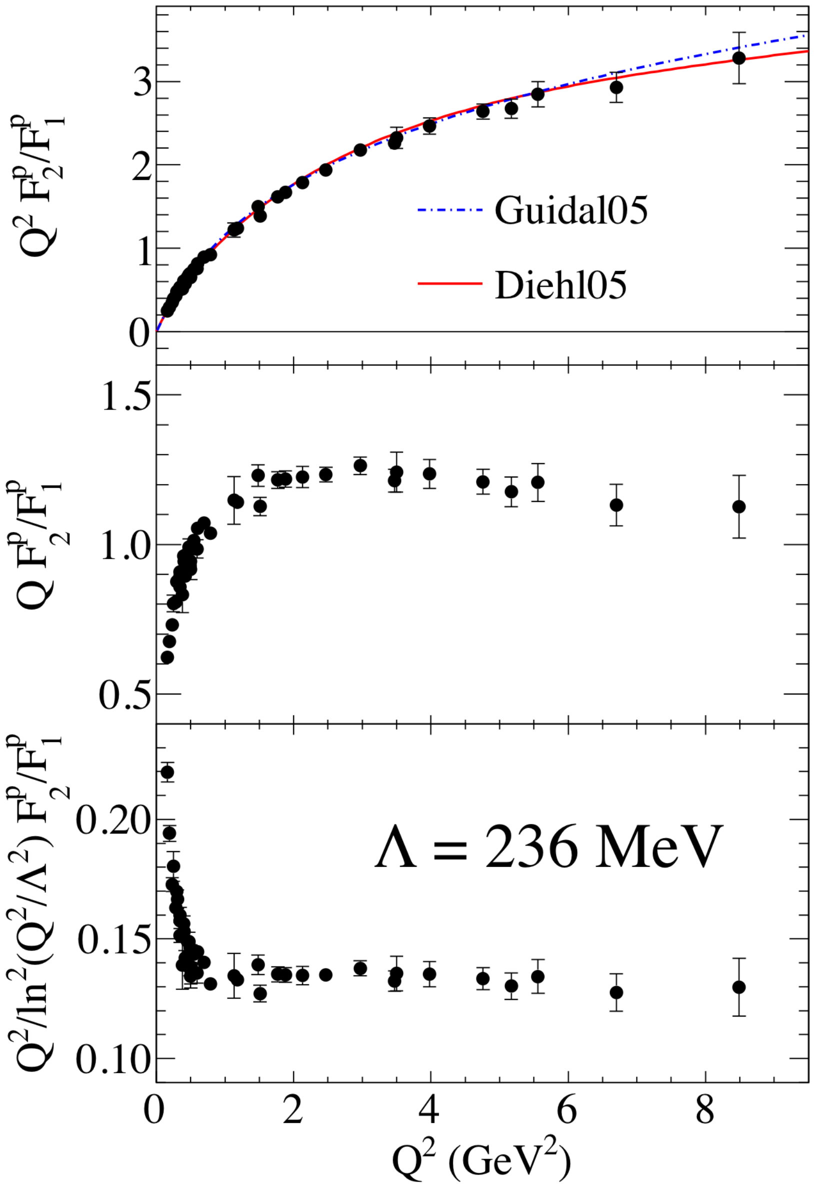

$$G_E \equiv F_1 - \tau F_2$$

$$G_M \equiv F_1 + F_2$$

$$F_1 = \frac{G_E + \tau G_M}{1+\tau}$$

$$F_2 = \frac{G_M - G_E}{1+\tau}$$

$$\frac{F_2}{F_1} = \frac{1 - \frac{G_E}{G_M}}{\tau + \frac{G_E}{G_M}}$$

- The measurement of the ratio $\frac{G_E}{G_M}$ to high Q^2 is equivalent to a measurement of the Pauli/Dirac FF ratio $\frac{F_2}{F_1}$. The precise determination of F_2 provides an important constraint, via model-independent sum rules, on the high-x/high-t behavior of the tensor GPD E(x,t) that is presently only poorly constrained by existing measurements of DVCS observables. This in turn contributes to the evaluation of the Ji sum rule for the total angular momentum carried by quark flavor *q*:

$$J_q = \frac{1}{2}\int_{-1}^{+1} dx x [H^q(x,\xi,t=0) + E^q(x,\xi,t=0)].$$

"Role of diquark correlations and the pion cloud in nucleon elastic form factors"

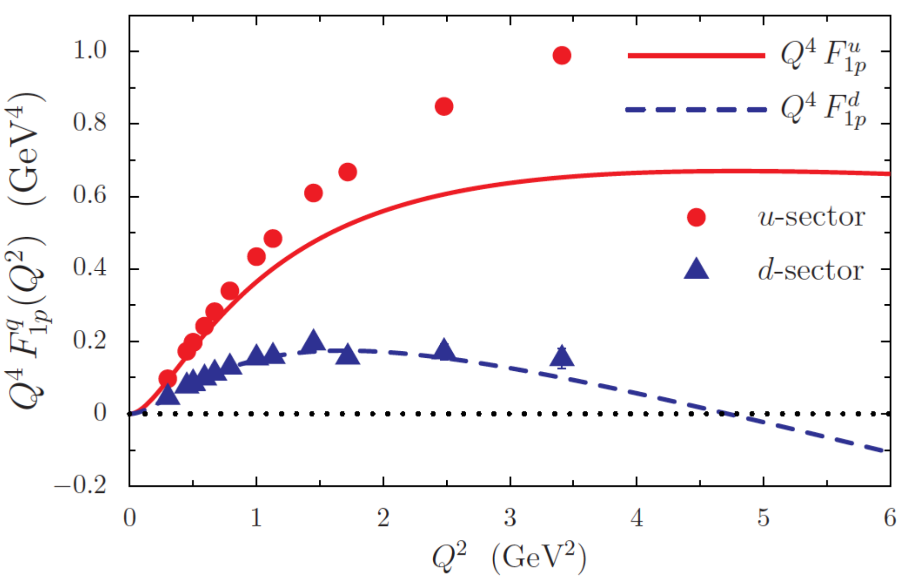

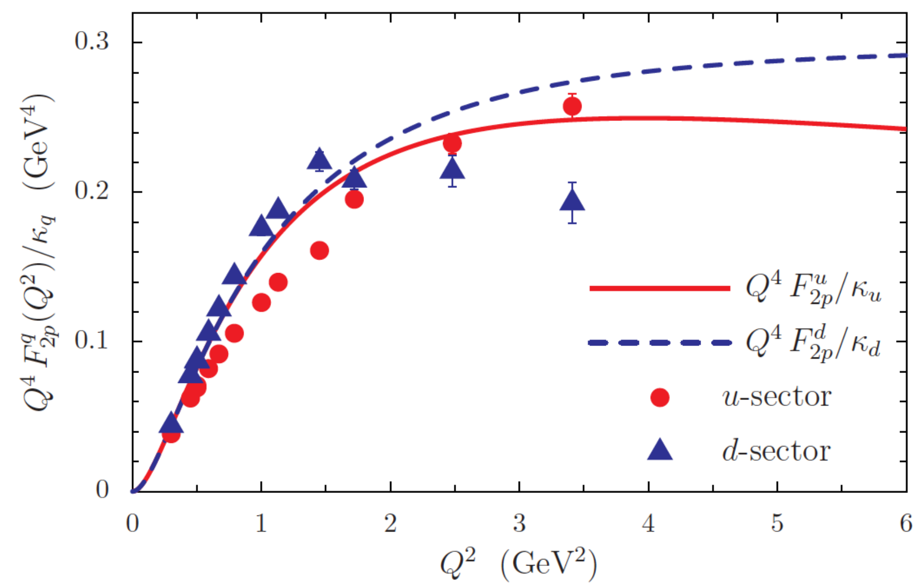

I. Cloet, W. Bentz and A. Thomas: Phys. Rev. C 90, 045202 (2014)

- Nucleon EMFF calculation in covariant, confining NJL model
- Parameter-free calculation (no fit to form factors)
- Softness of d-quark Dirac FF a consequence of dominance of scalar diquark correlations in nucleon wavefunction
- Axial vector diquark correlations and pion cloud effects play a more significant role in the Pauli form factors

Two-photon-exchange and the G_{Ep} puzzle—experiment and theory

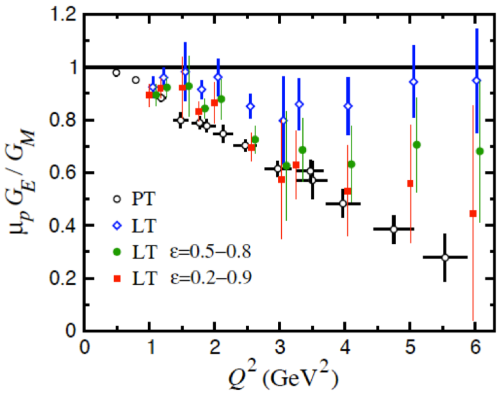

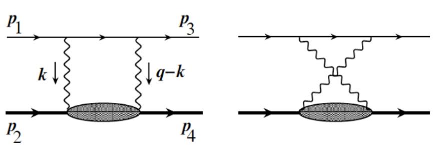

FIG. 1: Two-photon exchange box and crossed box diagrams for elastic electron–proton scattering.

"Hadronic" approach: Blunden, Melnitchouk, Tjon, **PRC 72, 034612 (2005)**. TPEX corrections with N intermediate state

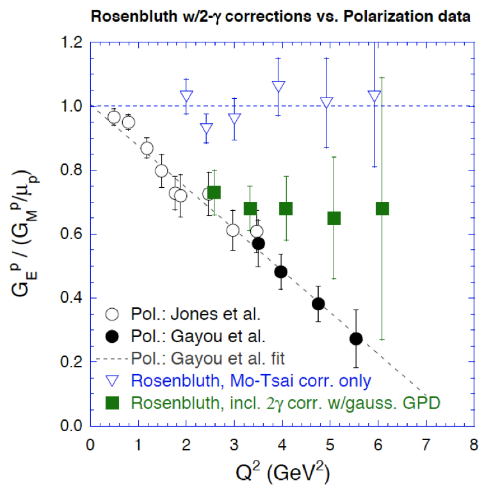

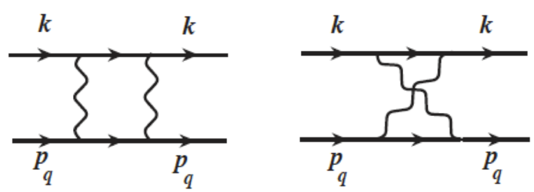

"Partonic" approach: Afanasev *et al.*, **PRD 72, 013008 (2005).** TPEX in "hard" scattering on a single quark, embedded in nucleon through GPDs

Experimental efforts:

- Several experimental observables are directly sensitive to TPEX effects
- ε-dependence of "R" ratio from polarization transfer. GEp-2γ: originally published Meziane *et al.*, **PRL 106, 132501 (2011),** and this work
- Induced normal recoil polarization or analyzing power A_N; imaginary part of TPEX amplitude—**never measured!**
- Elastic e^+p/e^-p cross section ratio: zero in one-photon exchange, measures real part of 2γ-exchange amplitude. Three experiments recently published:
    - CLAS-TPE (JLab Hall B)
    - OLYMPUS@DESY
    - VEPP-III (Novosibirsk)
- For a recent review, see Afanasev *et al.*, Prog. Part. Nucl. Phys. 95,245(2017)

GEp-2γ data compared to model TPEX calculations

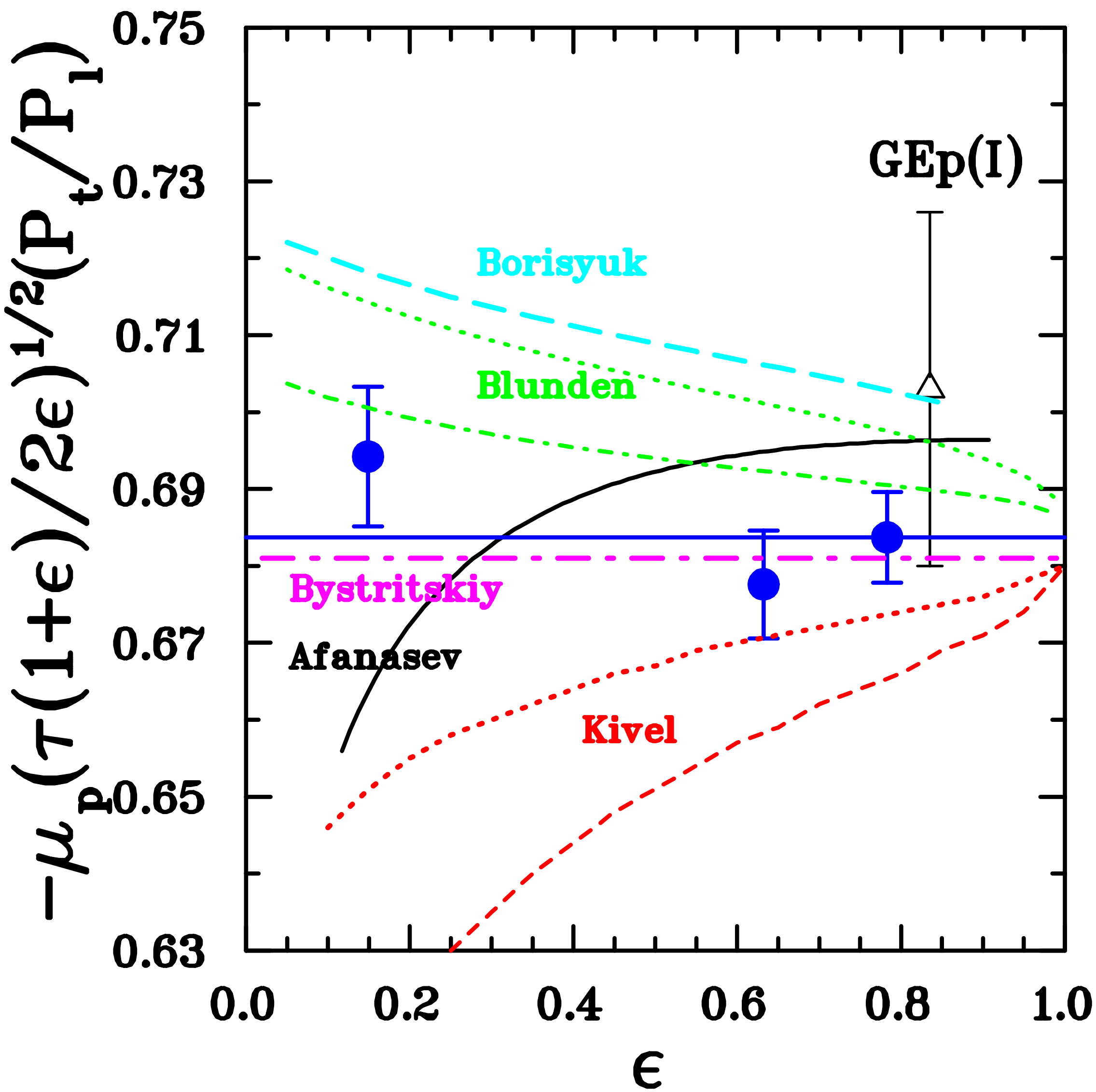

- Borisyuk: Phys. Rev. C 89, 025204 (2014).
  - Dispersion theory calculation including P_{33} πN contribution with width, shape, and nonresonant continuum
- Blunden: Phys. Rev. C95, 065209 (2017)
  - Dispersion theory calculation with "on shell" intermediate N (green dot-dashed) and N+Δ (green dotted)
- Bystritskiy: Phys. Rev. C75, 015207 (2007).
  - All-order QED RC calculation using electron structure function method
- Afanasev: Phys. Rev. D72, 013008 (2005).
  - Partonic approach using GPD model
- Kivel: Phys. Rev. Lett. 103, 092004 (2009)
  - PQCD approach using DAs

How to reach higher Q^2?

- Elastic ep cross section scales as $\sigma \approx E^2/Q^{12}$
- FPP efficiency is roughly Q^2-independent
- FPP analyzing power scales roughly as $1/p_p \sim M/Q^2$
- Statistical FOM scales as $NA_y^2 \sim E^2/Q^{16}$
- Increase beam polarization? 80%→100% would only increase FOM by 1.6
- Increase luminosity? Best possible at JLab 12 GeV ~ 10^{39} cm^{-2} s^{-1}; ~factor of 2 above 6 GeV expt's.
- Most room for growth? →***Increase solid angle/Q^2 acceptance!***
  - **2X increase in target thickness and solid angle from 6→35 msr leads to ~30X gain in figure-of-merit**
- JLab PAC-approved G_E^p experiment: E12-07-109; 45 days in Hall A
  - $\Delta(\mu G_E/G_M) \sim 0.07$ @$Q^2 = 12$ GeV^2

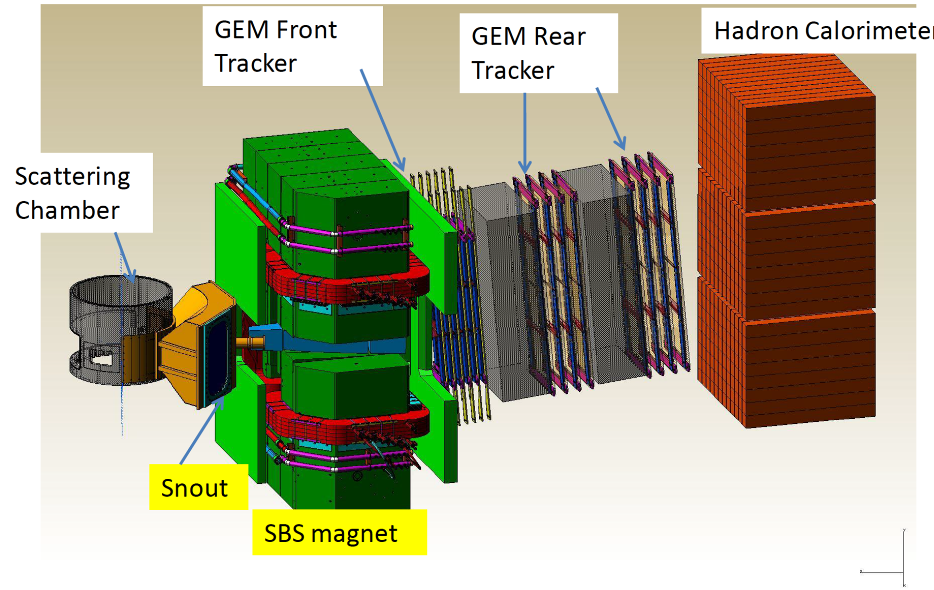

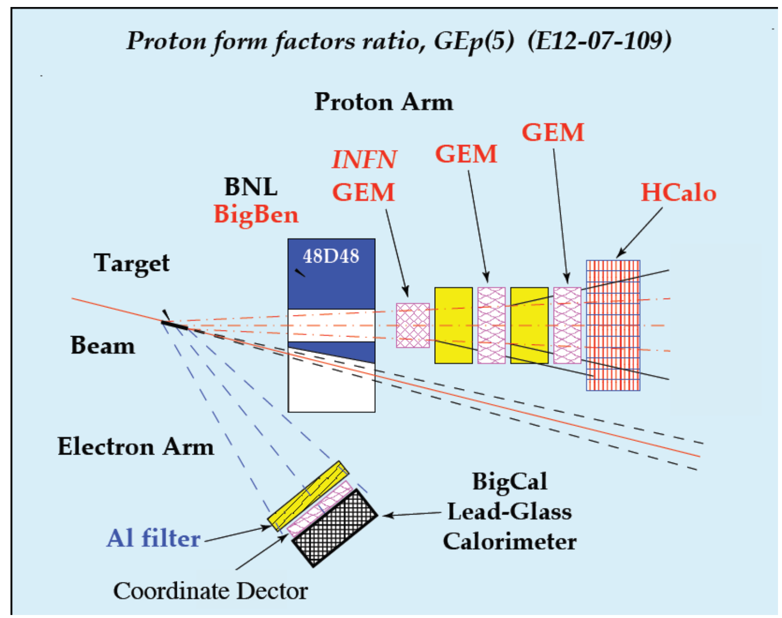

Statistical FOM of polarization transfer expt.'s

Experiment	Q^2 $(\mathrm{GeV/c})^2$	E_e (GeV)	$\Delta\Omega_p$ (msr)	P_e (%)	$\Delta\left(\mu_p G_E^p / G_M^p\right)$	Reference
GEp-I	0.5-3.5	0.9-4.1	6.5	40-60	0.01-0.05	PRL **84**, 1398 (2000), PRC **71**, 055202 (2005)
GEp-II	3.5-5.6	4.6	6.5	70	0.05-0.09	PRL **88**, 092301 (2002) PRC **85**, 045203 (2012)
GEp-III	5.2-8.5	4.0, 5.7	7	80-85	0.07-0.18	PRL **104**, 242301 (2010)

Previous PT experiments: focusing magnetic spectrometers, small proton solid angle/ΔQ^2

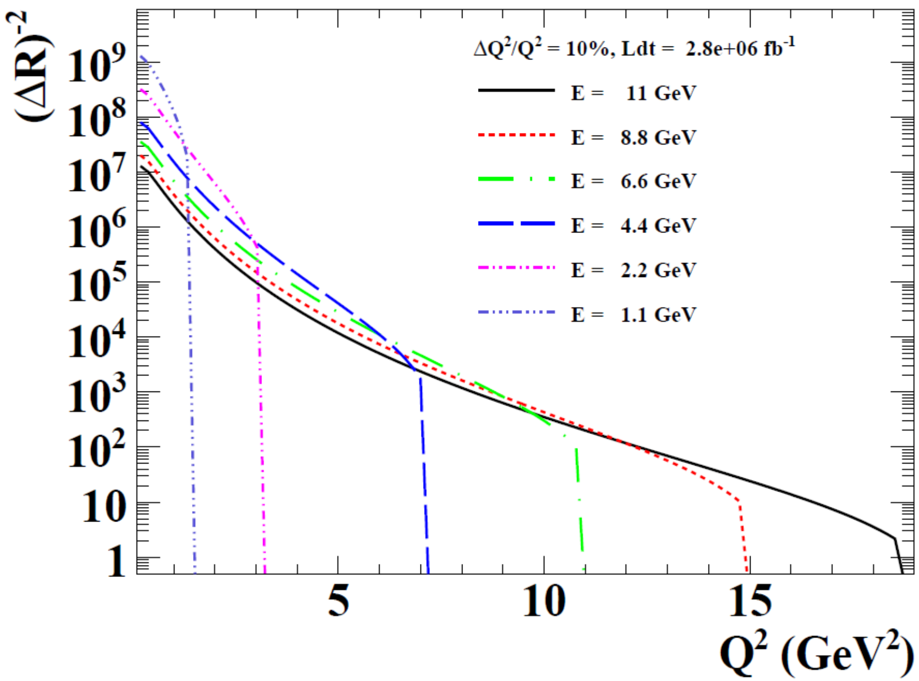

Theoretical PT FOM vs. Q^2 for different beam energies

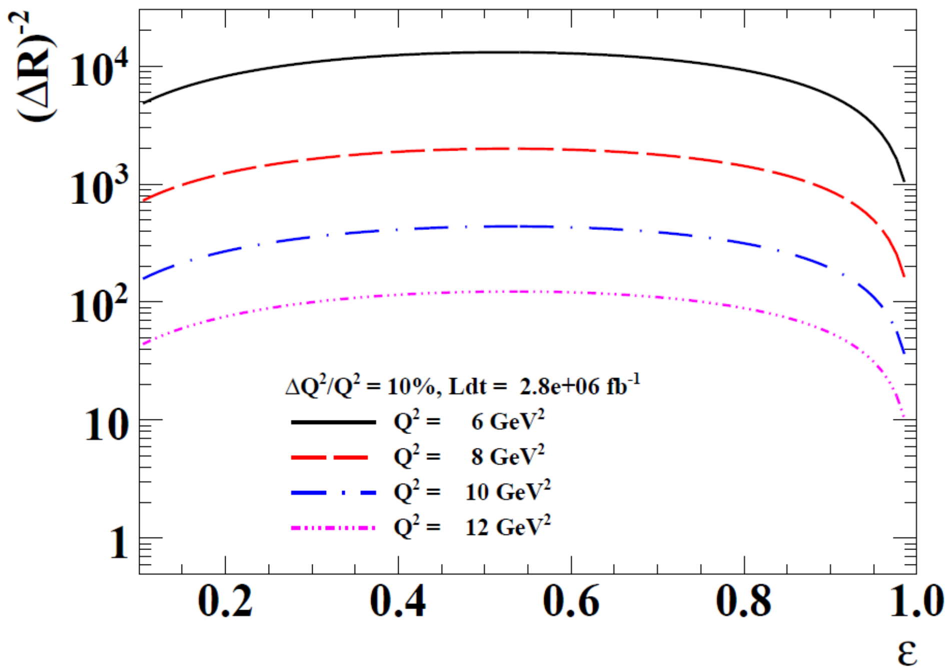

Theoretical PT FOM vs. ε at various Q^2 values

Polarization Transfer FOM vs. Q^2: HMS/HRS vs SBS

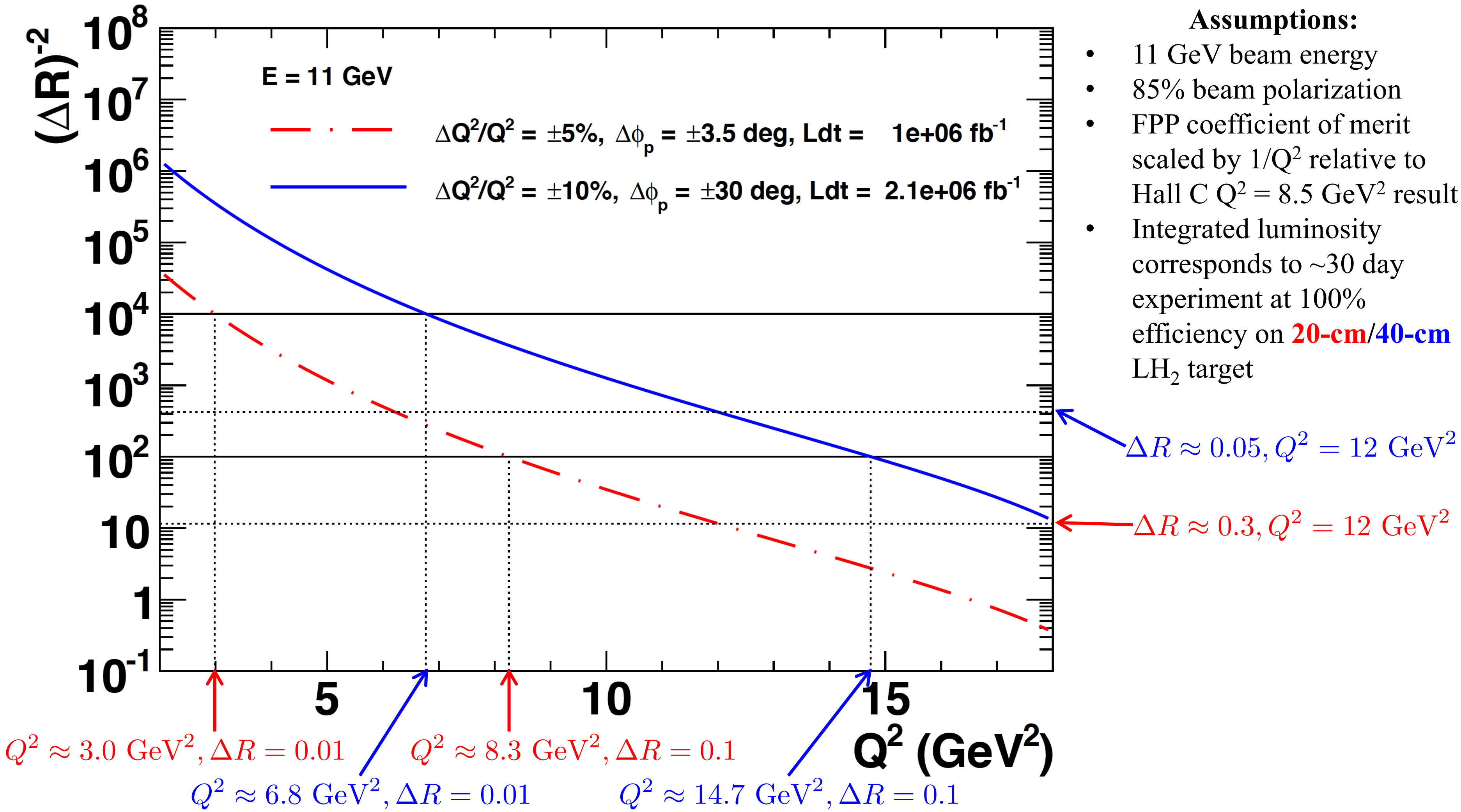

Assumptions:

- 11 GeV beam energy
- 85% beam polarization
- FPP coefficient of merit scaled by $1/Q^2$ relative to Hall C $Q^2 = 8.5$ GeV^2 result
- Integrated luminosity corresponds to ~30 day experiment at 100% efficiency on **20-cm**/**40-cm** LH_2 target

Increase in proton solid angle from 6→35 msr and ~2X increase in luminosity leads to *doubling* of Q^2 range for which absolute $\Delta(\mu G_E/G_M) \leq 0.1$